

CERAMIDE ACCUMULATION IN THE ALPHA CELL DRIVES GLUCAGON SECRETION AND
HYPERGLYCEMIA

APPROVED BY SUPERVISORY COMMITTEE

Chair, Examining Committee
(Jeffrey McDonald, Ph.D.)

(Michael Roth, Ph.D.)

(Philipp Scherer, Ph.D.)

(Roger Unger, M.D.)

CERAMIDE ACCUMULATION IN THE ALPHA CELL DRIVES GLUCAGON SECRETION AND
HYPERGLYCEMIA

by

MACKENZIE JO PEARSON

DISSERTATION

Presented to the Faculty of the Graduate School of Biomedical Sciences

The University of Texas Southwestern Medical Center at Dallas

In Partial Fulfillment of the Requirements

For the Degree of

DOCTOR OF PHILOSOPHY

The University of Texas Southwestern Medical Center at Dallas

Dallas, Texas

May 2017

Copyright

by

Mackenzie Jo Pearson, 2017

All Rights Reserved

Ceramide Accumulation in the Alpha Cell Drives Glucagon Secretion and Hyperglycemia

Mackenzie Jo Pearson, PhD

The University of Texas Southwestern Medical Center at Dallas, 2017

William Holland, PhD

Lipids were not always considered to be biologically active compounds. For many years, researchers believed they served two purposes—to act as building blocks of membranes and to serve as an energy source. Yet, it wasn't until the early 1960's that Bergstrom, Samuelsson and others, discovered that the hormone-like prostaglandins were derived from arachidonate—an essential free fatty acid. Since this biosynthetic precursor has many roles in metabolic processes, researchers gained interest in the functions that lipids and their metabolites might play in other cellular processes (William W. Christie AOCs Lipid Library).

In 1994 that Roger Unger and collaborators coined the term “lipotoxicity”. Their research described a lipid overload in pancreatic beta-cells that results in a lipid-induced dysfunction that ultimately leads to programmed cell death (1). More importantly, their later research in ZDF diabetic fatty rats showed an increase in serine palmitoyl transferase, the rate limiting enzyme in ceramide synthesis, in islets of obese fa/fa ZDF rats compared to lean mice of the same age (2). Blockade of ceramide synthesis in these islets demonstrated a decrease in lipid mediated apoptosis. Further studies have shown that aberrant deposition of ectopic lipid in peripheral tissues has been correlated to many metabolic disorders, cancers, heart

disease, and atherosclerosis. In 1998, Summers and group were able to show that de novo ceramide synthesis inhibits insulin stimulated glucose uptake in cultured adipocytes. From this study, they were able to show indirect inhibition of AKT to promote insulin resistance in a ceramide dependent manner (3). However, does ceramide accumulation specifically within the alpha-cell play a role in the diabetic phenotype?

In 1975, Drs. Unger and Orci proposed a bihormonal-abnormality hypothesis. To perpetuate hyperglycemia in the diabetic state, not only must there be deficient amounts of insulin available, but also excessive amounts of glucagon present. They were the first to provide evidence that hyperglucagonemia in type 2 diabetes mellitus may result from insulin resistant alpha-cells, since patients' circulating glucagon levels were poorly suppressed by exogenous insulin. Additionally, the Kulkarni group demonstrated that *in vitro* and *in vivo* deletion of the insulin receptors within alpha-cells caused insulin resistance, facilitated hyperglucagonemia, and perpetuated hyperglycemia. I hypothesize that ablating ceramide accumulation within the alpha-cell can improve insulin signaling or regulate glucagon secretion in this cell type. To investigate the possible mechanisms by which glucagon is regulated, three mouse models have been generated. Acid ceramidase (AC) overexpression, adiponectin receptor 2 (AdipoR2) overexpression, and FGF21 signaling impairment by deletion of its coreceptor beta-klotho are the three novel approaches outlined in this body of work to elucidate the effects of ceramides on glucagon secretion.

DEDICATION

To my parents George and Tanya Pearson,
my sister Megan and favorite brother-in-law Hamish,
my grandparents Ron and Pam Robbins,
my aunt and uncle Teena Robbins and Joe Licata,
and to my best friend Emily Berry.

ACKNOWLEDGMENTS

First and foremost, there is not enough gratitude in the world to express how thankful I am to my mentor and friend, Dr. William Holland. You took in an analytical chemist, taught me biology, put up with my sass, and we accomplished some amazing science in the process. Thank you for allowing me to train in your lab. The knowledge base I gained will invaluablely aid me in my future career. Nothing will ever take place of the late night writing sessions, weekends in the mouse house, or dinners and drinks to keep our sanity. Again, thank you, Good Dude.

My thesis committee members, Jeff McDonald, Michael Roth, Philipp Scherer and Roger Unger, your guidance and knowledge through these years shaped me into the scientist I am today. Thanks you for challenging me and pushing me to be a better scientist.

A special thanks to Ruth Gordillo. Your support, both scientifically and mentally, kept me sane during long days and late nights in the lab. Thank you to our support staff, Kristen Dyer for always providing a listening ear and Cyndi Fairfield for always making my life easier.

Chelsea Hepler, your friendship these last few years was invaluable. You were always there when I needed support, a chat, or a beer. Cheers to many more to come. Ashely Anderson, Genaro Hernandez, and Brandt Nichols—if it wasn't for you guys I don't know if I would have stayed. Thomas Morley, a sincere thank you for always keeping me on the level and for your scientific advice.

My warmest wishes and gratitude goes out to my lab mates, Joshua Johnson, Zeke Quittner-Strom, and Ankit Sharma. Your relentless efforts in the lab help me graduate and

thanks for all the laughs. Also, my gratitude goes to Angelica Sifuentes for supporting me through my first years in the lab.

Last but not least, I couldn't have done this without the support of my family. My parents, George and Tanya, deserve a medal for getting me here. Your constant support, stubbornness, questions, and love got me to where I am today. My sister, Megan, I truly believe if it weren't for you I would have never gotten to where I am today. Your example, friendship, and sisterly competitiveness drove me to always be my better self. Hamish—thanks for always letting me think that I am smarter than you. And a special thanks to the girl who is like a sister to me, Emily Berry. Even though we were always miles apart your support was never more than a phone call away.

TABLE OF CONTENTS

PRIOR PUBLICATIONS.....	X
LIST OF FIGURES.....	XI
LIST OF ABBREVIATION	XIII
CHAPTER 1: Introduction	1
Clinical Trials, Triumphs and Tribulations of Glucagon Receptor Antagonists... ..	2
References	10
CHAPTER 2: Ceramide Accumulation in the Alpha Cell Drives Glucagon Secretion and Hyperglycemia... ..	13
Abstract.....	14
Introduction	14
Results.....	16
Discussion.....	24
Acknowledgements.....	26
References	27
Methods And Materials:	29
CHAPTER 3: Conclusions and Future Directions	46
Abstract.....	46
Introduction	46
Results.....	48
Discussion.....	51
Methods And Materials:	54
References	58

Prior Publications

Xia J, Holland WL, Johnson J, Kai Sun, Pearson M, Sharma AX, Quittner-Strom E, Tippetts T, Gordillo R, Scherer PE. *Inducible Overexpression of Adiponectin Receptors Highlight the Roles of Adiponectin-Induced Ceramidase Signaling in Lipid and Glucose Homeostasis. Molecular Metabolism, In Press.*

Fujikawa, T., Castorena, C. M., **Pearson, M.**, Kusminski, C. M., Ahmed, N., Battiprolu, P. K., ... Elmquist, J. K. (2016). SF-1 expression in the hypothalamus is required for beneficial metabolic effects of exercise. *eLife*, 5, e18206. <http://doi.org/10.7554/eLife.18206>

Pearson, M., Unger R.H. Holland, W.L., Clinical Trials, Triumphs, and Tribulations of Glucagon Receptor Antagonists. *Diabetes Care* Jul 2016, 39 (7) 1075-1077; **DOI:** 10.2337/dci15-0033

Amosii, L., Holland, W., Sanchez-Ortiz, E., Baskin, K. K., **Pearson, M.**, Burgess, S. C., ... Olson, E. N. (2016). A MED13-dependent skeletal muscle gene program controls systemic glucose homeostasis and hepatic metabolism. *Genes & Development*, 30(4), 434–446. <http://doi.org/10.1101/gad.273128.115>

Xia, J. Y., Holland, W. L., Kusminski, C. M., Sun, K., Sharma, A. X., **Pearson, M. J.**, ... Scherer, P. E. (2015). Targeted Induction of Ceramide Degradation Leads to Improved Systemic Metabolism and Reduced Hepatic Steatosis. *Cell Metabolism*, 22(2), 266–278. <http://doi.org/10.1016/j.cmet.2015.06.007>

Duarte, J. A. G., Carvalho, F., **Pearson, M.**, Horton, J. D., Browning, J. D., Jones, J. G., & Burgess, S. C. (2014). A high-fat diet suppresses de novo lipogenesis and desaturation but not elongation and triglyceride synthesis in mice. *Journal of Lipid Research*, 55(12), 2541–2553. <http://doi.org/10.1194/jlr.M052308>

List of Figures

CHAPTER 1

Figure 1: The Bihormonal Regulation of Glucose	12
--	----

CHAPTER 2

Figure 1: Ceramide Promotes Glucagon Production and Secretion In Vitro and Ex Vivo	35
--	----

Figure 2: Acid ceramidase overexpression in the α -cell improves α -cell insulin action in lean mice	36
--	----

Figure 3: Alpha-cell overexpression of acid ceramidase enhances suppression of glucagon in diet-induced obesity.	37
---	----

Figure 4: Induction of acid ceramidase in the α -cell improves insulin sensitivity after long-term high-fat diet exposure	38
--	----

Figure 5: Overexpression of acid ceramidase in the α -cell of Lepob/ob mice prevents hyperglycemia and hyperglucagonemia.	39
---	----

Figure 6: Inducing acid ceramidase overexpression in the α -cell of obese diabetic mice reverses hyperglycemia	40
---	----

Supplement Figure 1 in support of Fig. 1	41
--	----

Supplement Figure 2 in support of Fig. 2	42
--	----

Supplement Figure 3 in support of Fig. 3..... 43

Supplement Figure 4 in support of Fig. 4..... 44

Supplement Figure 5 in support of Fig. 5..... 45

CHAPTER 3

Figure 1: Adiponectin ameliorates hyperglycemia and hyperglucagonemia via induction of ceramidase activity59

Figure 2: FGF21 independently degrades ceramides and blunts glucagon secretion In Vitro 60

Figure 3: Alpha cell specific deletion of the FGF21 coreceptor, beta-klotho, exhibits increases in circulating factors..... 61

Figure 4: Diet Induced Obesity decreases insulin sensitivity in beta-klotho deficient knockout mice..... 62

Supplement Figure 1 in support of Fig. 1..... 63

List of Abbreviations

APN – adiponectin

AdipoR – adiponectin receptor

AMPK – AMP-activated protein kinase

C1P – ceramide-1-phosphate

DAG – diacylglycerol

DIO – diet induced obesity

Dox- doxycycline

FFAs- free fatty acids

FGF21- fibroblast growth factor 21

gWAT- gonadal white adipose tissue

het- heterozygous

HFD – high fat diet

HFD-dox – high fat diet with dox

ITT- insulin tolerance test

KO- knockout

OGTT- oral glucose tolerance test

PKC – protein kinase C

PPAR γ – peroxisome proliferator activated receptor

rtTA- reverse tetracycline transactivator

S1P- sphingosine-1-phosphate

STZ- streptozotocin

SPT – serine palmitoyl-CoA transferase

TG- triglyceride

TNF- α – tumor necrosis factor alpha

TLR4 – toll like receptor 4

TRE- tetracycline response element

TZD- thiazolidinediones

WT- wildtype

Chapter 1

Title: Clinical Trials, Triumphs and Tribulations of Glucagon Receptor Antagonists

Running title: Glucagon Receptor Antagonists

Mackenzie J. Pearson^a, Roger H. Unger^{a,b} and William L. Holland^a

^aTouchstone Diabetes Center, Department of Internal Medicine. University of Texas Southwestern Medical Center, Dallas TX. 75390 USA

^bVA North Texas Health Care System, Dallas, TX 75216, USA

Corresponding Author:

William L. Holland Ph.D.

UT Southwestern Medical Center

5323 Harry Hines Blvd.

Dallas, TX 75390-8549

Phone: 214-648-2566

Fax: 214-648-8720

Email: william.holland@utsouthwestern.edu

The following chapter is from the publication: Diabetes Care 2016 Jul; 39(7): 1075-1077. <https://doi.org/10.2337/dci15-0033>

ABSTRACT

Since the discovery of glucagon's opposing actions to insulin in 1959, drugs targeting the inhibition of glucagon action have been pondered. In recent years, several attempts to generate small molecules or antibodies which impair glucagon action have been pursued as potential therapeutics for Type 2 Diabetes. Recently Kazda and colleagues summarized the outcomes of the phase 2a and phase 2b clinical trials of LY2409021, a small molecule glucagon receptor antagonist (GRA). This is the largest and longest trial for safety and efficacy of a GRA ever performed. Importantly, LY2409021 does not produce side effects on cholesterol homeostasis that have impeded the progress of other small molecule GRAs. Here, I place their success in perspective, and discuss the advantages and concerns relating to glucagon-based therapeutics, as this line of drugs comes closer than ever to achieving their clinical potential.

Clinical Trials, Triumphs, and Tribulations of Glucagon Receptor Antagonists

In 1922 the first children with type-1 diabetes were treated with an insulin-containing pancreatic extract, preventing ketoacidosis and an insidious death. In addition to the discovery of insulin, the crew of Banting, Best and Collip observed glucagon action, as they had noticed in their preclinical studies in canines that some of their crude insulin preparations would raise glucose levels in the dog briefly before glucose was lowered (1; 2). This glucose raising peptide was termed “glucagon”(3) and subsequently purified and identified as a 29 amino acid peptide (4). In 1959, the development of the radioimmunoassay made it possible to quantify the two major glucoregulatory hormones, insulin (5) and glucagon (6). It was quickly established that glucagon was in fact a true hormone responsible for maintaining the glucose supply to the brain via increased glycogenolysis and gluconeogenesis.

It has since been demonstrated that every form of diabetes is associated with hyperglucagonemia, the suppression of which eliminated the hyperglycemia (7). Following pancreatectomy, glucagon-producing alpha cells proliferate in the fundus of the stomach allowing hyperglucagonemia (8). In other words diabetes is a bihormonal disease rather than simply the result of insulin deficiency (**Figure 1**) (9). It was further shown that glucagon-producing alpha cells are topographically arranged for functional reasons with 91% of alpha cells in the islets of Langerhans juxtaposed to beta cells. This close proximity permits insulin to tightly regulate glucagon secretion and precisely control the insulin/glucagon ratio in the healthy pancreatic islet. When insulin is present, the alpha cells, juxtaposed to beta cells,

receive the highest insulin concentration of any target cell in the body. The paracrine levels of insulin reaching alpha cells have been estimated at between 2000 and 4000 μ Units /ml(10). This is almost impossible to achieve by administration of insulin into the periphery, which provides a substantial gap in our ability to treat diabetes effectively within the clinic. An alternative to higher doses of insulin for the treatment of hyperglycemia is to minimize the contributions of glucagon. Thus, the insulin:glucagon ratio is enhanced by minimizing the denominator and glucagon's effects on the liver.

Regulation of glucagon secretion occurs locally, within the islet, and via effects in the central nervous system(11). Insulin, gamma-aminobutyric acid (GABA) and leptin, are potent physiologic regulators that dampen glucagon secretion(12). In 1984 Unger et al. conducted experiments that demonstrated the paracrine role of insulin on α -cell function (10). Using a potent anti- insulin neutralizing serum, they perfused normal pancreata and showed that when insulin inside the islet was neutralized, glucagon levels rose by 150% and remained elevated until the anti- serum was stopped. Ablation of insulin receptor from the alpha cell has supported the importance of insulin as a negative regulator of alpha cell secretion(13; 14).

Glucagon raises blood glucose through its cognate receptor in the liver [reviewed in (15)]. This G-protein-coupled receptor is responsible for driving gluconeogenesis by up-regulating glucose-6-phosphatase (G6PC) and phosphoenolpyruvate carboxykinase (PEPCK), key enzymes which are activated through adenylyl cyclase signaling to protein kinase A (PKA) and subsequently cAMP response element-binding protein (CREB) and peroxisome proliferator-activated receptor γ -coactivator-1 (PGC1a). Salt inducible kinase 2 (SIK2) is also activated through PKA. SIK2 phosphorylates and activates CREB regulated transcription co-activator 2

(CRTC2), another co-transcriptional regulator of gluconeogenic genes. By blunting glucagon action on the liver these signals are diminished, and hepatic glucose efflux is reduced.

Since the discovery of glucagon's counter-regulatory effects to oppose the glucose-lowering actions of insulin, strategies for blunting glucagon secretion or glucagon action have been imagined as potential therapies for diabetes. Over the last decade, several glucagon receptor antagonists (GRAs) have emerged from the pharmaceutical industry and have been evaluated both preclinically and in clinical trials. These approaches have included small molecule antagonists, which can work through allosteric or competitive inhibition; fully human antibodies, which assuages side effects from chimeric or humanized antibodies against glucagon receptor; and antisense oligonucleotides to downregulate the expression of the glucagon receptor. All of these appear to have glucose-lowering properties and have been recently reviewed (16).

Christof Kazda and colleagues described the most recent clinical trials by Eli Lilly and company using their small molecule GRA (LY2409021). The initial randomized, double-blind phase 2a clinical study compared the effects of 3 doses of LY2409021 with placebo over a 12-week study period. Patients were either naïve to antidiabetic medications or on metformin (59%). Dose-dependent lowering of HbA1c was achieved with 10, 30, or 60 mg of LY2409021, while HbA1c rose 11% in patients receiving placebo. Fasting blood glucose and self-monitored blood glucose were lowered by all 3 doses. During the phase 2b study, 2.5, 10 or 20 mg doses of LY2409021 produced a dose-dependent improvement in glycemia at the two higher doses, that was sustained for the 24-week treatment period. One-

third of patients achieved HbA1c levels below 6.5% and half of the patients achieved HbA1c levels below 7%. Dose dependent increases in total glucagon-like peptide-1 (GLP-1) and ALT were observed and returned to basal levels during a post-treatment washout period. No significant changes in body weight, blood pressure, heart rate, ECG, or plasma lipid were detected for any dose of LY2409021 as compared to the placebo control group.

The involvement of GLP-1 has been investigated as a contributor to GRA-mediated improvements in glucose metabolism. As glucagon and GLP-1 are derived from the same preproglucagon precursor, endocrine feedback stemming from blunted glucagon action prompts increases in both GLP-1 and glucagon production from the alpha cell. In preclinical models both fibroblast growth factor 21 (FGF21) and GLP-1 are known to increase after GRA treatment. Although data have suggested that these hormones may contribute to the glycemic improvements evoked by GRAs(17; 18), conflicting results exist(19) (Wang and Unger unpublished observations). LY2409021 did not alter levels of active GLP-1, suggesting that it is dispensable for the glycemic improvements in humans.

Several concerns with previous GRAs have been noted. These include increased serum cholesterol, increases in body weight, glycogen storage alterations, enhanced alpha cell hyperplasia, and increases in serum transaminase levels. The most obvious concern to most clinicians is an enhanced risk of hypoglycemia. No severe hypoglycemic episodes occurred in this study. During phase 2a 4 symptomatic hypoglycemic events were reported. Overall, the incidence of hypoglycemia was not statistically different from placebo. Importantly, exogenous glucagon can still rescue patients treated with LY2409021, as its affinity for the

glucagon receptor is still low enough to allow increased glycemia following intramuscular injection of glucagon.

An important critique overcome by this work is the fear that all GRAs will cause increases in serum lipids. Most notably, Merck's small molecule GRAs revealed increases in LDL cholesterol during phase 2 clinical trials. It is reasonable to speculate that insulin may drive lipogenesis (through sterol response binding protein 1c) more strongly in the absence of glucagon action, during the acute period before insulin secretion wanes to match the decreased demand for insulin. Rather, the Merck team showed that their small molecule, MK-0893, increases cholesterol absorption while lowering blood glucose (20). Importantly, LY2409021 did not increase LDL, and data trended toward improvements in cholesterol.

Another concern of GRA therapy would be the development of glycogen storage disease. In mice, a 4-fold increase of glycogen has been reported in glucagon receptor null mice (21). With LY2109021, changes were not seen in rodents, but were noted in cynomolgus monkeys(22). This will be important to investigate as it may offer a potential explanation for the elevated ALT levels. Notably, most glycogen storage diseases present with elevated ALT and AST. Glycogen content in human subjects has not been reported yet with this candidate drug.

Increased liver enzymes are perhaps the most commonly observed side effect of GRA treatment. Three of the 85 patients in this study showed ALT levels >3X the upper limit of normal. AST also increased, albeit, to a lesser degree. In the phase 2b study, 8 of the 191 patients showed increases in ALT which exceeded 3 times the upper limit of normal. FDA guidelines for Drug Induced Liver Injury (DILI) are defined by an ALT/AST increase by 3X, with

concurrent increases in Alkaline Phosphatase (AKP) by 2X, and Total Bilirubin by 2X. None of the subjects with high ALT levels showed concomitant increases in bilirubin, AKP, or symptoms of liver disease. It is possible that increased glycogen content may account for some changes in liver enzymes. Alternatively, this may be driven by an alternative means of handling the amino acids which would otherwise be used for gluconeogenesis. Regardless, the small degree of change in AST/ALT, in the absence of other markers of liver toxicity (alkaline phosphatase or bilirubin), suggest that these drugs would not exceed FDA guidelines for drug-induced liver injury.

The most severe concern with GRA therapy is malignant transformation of alpha cells, as they undergo marked hyperplasia when the action of their secretory product is blocked. Since glucagon promotes depletion of amino acids by stimulating their use as gluconeogenic substrates (23), GRAs promote an increase in hepatic and circulating amino acids. In turn, this can lead to enhanced alpha cell proliferation by enhancing mTOR activation within the alpha cell (24). While the Unger and Holland groups have yet to encounter a glucagonoma in any of the animals treated chronically with glucagon receptor antibody, the disease (glucagonoma) is such a terrible one that one may consider monitoring patients treated with GRAs. A very early marker of glucagonoma is easily detectable by monitoring a c-terminal extension of the glucagon molecule.

An exciting direction which remains underexplored is the potential for GRAs to treat type-1 diabetes. In rodent models that have been treated with antibodies against the glucagon receptor glycemic control improves far better than with insulin monotherapy alone (12). The primary advantage provided by the GRAs is the prevention of

glycemic volatility as oscillations in glucose are greatly minimized and glucose levels remain consistently between 80-120 mg/dL. LY2409021 has been revealed at conference proceedings to diminish the need for insulin in Type-1 diabetic patients. There is reason for optimism that GRAs will find their way into the clinic to provide a potent glycemic therapy for the treatment of diabetes mellitus(25).

REFERENCES

1. Banting FG, Best CH, Collip JB, Campbell WR, Fletcher AA: Pancreatic Extracts in the Treatment of Diabetes Mellitus. Canadian Medical Association journal 1922;12:141-146
2. Best CH: Personal Communication. Unger RH, Ed., 1959
3. Kimball C.P. and Merlin JR: Some precipitation reactions of insulin. The Journal of biological chemistry 1923;58:337-348
4. Staub A, Sinn L, Behrens OK: Purification and crystallization of glucagon. The Journal of biological chemistry 1955;214:619-632
5. Berson SA, Yalow RS: Quantitative aspects of the reaction between insulin and insulin-binding antibody. The Journal of clinical investigation 1959;38:1996-2016
6. Unger RH, Eisentraut AM, Mc CM, Keller S, Lanz HC, Madison LL: Glucagon antibodies and their use for immunoassay for glucagon. Proceedings of the Society for Experimental Biology and Medicine Society for Experimental Biology and Medicine 1959;102:621-623
7. Raskin P, Unger RH: Hyperglucagonemia and its suppression. Importance in the metabolic control of diabetes. The New England journal of medicine 1978;299:433-436
8. Sasaki H, Rubalcava B, Baetens D, Blazquez E, Srikant CB, Orci L, Unger RH: Identification of glucagon in the gastrointestinal tract. The Journal of clinical investigation 1975;56:135-145
9. Unger RH, Orci L: Paracrinology of islets and the paracrinopathy of diabetes. Proceedings of the National Academy of Sciences of the United States of America 2010;107:16009-16012
10. Maruyama H, Hisatomi A, Orci L, Grodsky GM, Unger RH: Insulin within islets is a physiologic glucagon release inhibitor. The Journal of clinical investigation 1984;74:2296-2299
11. Thorens B: Brain glucose sensing and neural regulation of insulin and glucagon secretion. Diabetes, obesity & metabolism 2011;13 Suppl 1:82-88
12. Wang MY, Yan H, Shi Z, Evans MR, Yu X, Lee Y, Chen S, Williams A, Philippe J, Roth MG, Unger RH: Glucagon receptor antibody completely suppresses type 1 diabetes phenotype without insulin by disrupting a novel diabetogenic pathway. Proceedings of the National Academy of Sciences of the United States of America 2015;112:2503-2508
13. Kawamori D, Kulkarni RN: Insulin modulation of glucagon secretion: the role of insulin and other factors in the regulation of glucagon secretion. Islets 2009;1:276-279
14. Kawamori D, Kurpad AJ, Hu J, Liew CW, Shih JL, Ford EL, Herrera PL, Polonsky KS, McGuinness OP, Kulkarni RN: Insulin signaling in alpha cells modulates glucagon secretion in vivo. Cell Metab 2009;9:350-361

15. Altarejos JY, Montminy M: CREB and the CRTC co-activators: sensors for hormonal and metabolic signals. *Nature reviews Molecular cell biology* 2011;12:141-151
16. Sammons MF, Lee EC: Recent progress in the development of small-molecule glucagon receptor antagonists. *Bioorganic & medicinal chemistry letters* 2015;25:4057-4064
17. Omar BA, Andersen B, Hald J, Raun K, Nishimura E, Ahren B: Fibroblast growth factor 21 (FGF21) and glucagon-like peptide 1 contribute to diabetes resistance in glucagon receptor-deficient mice. *Diabetes* 2014;63:101-110
18. Gu W, Winters KA, Motani AS, Komorowski R, Zhang Y, Liu Q, Wu X, Rulifson IC, Sivits G, Jr., Graham M, Yan H, Wang P, Moore S, Meng T, Lindberg RA, Veniant MM: Glucagon receptor antagonist-mediated improvements in glycemic control are dependent on functional pancreatic GLP-1 receptor. *American journal of physiology Endocrinology and metabolism* 2010;299:E624-632
19. Ali S, Lamont BJ, Charron MJ, Drucker DJ: Dual elimination of the glucagon and GLP-1 receptors in mice reveals plasticity in the incretin axis. *The Journal of clinical investigation* 2011;121:1917-1929
20. Guan HP, Yang X, Lu K, Wang SP, Castro-Perez JM, Previs S, Wright M, Shah V, Herath K, Xie D, Szeto D, Forrest G, Xiao JC, Palyha O, Sun LP, Andryuk PJ, Engel SS, Xiong Y, Lin S, Kelley DE, Erion MD, Davis HR, Wang L: Glucagon receptor antagonism induces increased cholesterol absorption. *Journal of lipid research* 2015;56:2183-2195
21. Lee Y, Berglund ED, Wang MY, Fu X, Yu X, Charron MJ, Burgess SC, Unger RH: Metabolic manifestations of insulin deficiency do not occur without glucagon action. *Proceedings of the National Academy of Sciences of the United States of America* 2012;109:14972-14976
22. Kelly RP, Garhyan P, Raddad E, Fu H, Lim CN, Prince MJ, Pinaire JA, Loh MT, Deeg MA: Short-term administration of the glucagon receptor antagonist LY2409021 lowers blood glucose in healthy people and in those with type 2 diabetes. *Diabetes, obesity & metabolism* 2015;17:414-422
23. Rocha DM, Faloona GR, Unger RH: Glucagon-stimulating activity of 20 amino acids in dogs. *The Journal of clinical investigation* 1972;51:2346-2351
24. Solloway MJ, Madjidi A, Gu C, Eastham-Anderson J, Clarke HJ, Kljavin N, Zavala-Solorio J, Kates L, Friedman B, Brauer M, Wang J, Fiehn O, Kolumam G, Stern H, Lowe JB, Peterson AS, Allan BB: Glucagon Couples Hepatic Amino Acid Catabolism to mTOR-Dependent Regulation of alpha-Cell Mass. *Cell reports* 2015;12:495-510
25. Kazda RPG, P.; Ding, Y., Kelly, R.P.; Hardy, T.A.; Kapitza, C. A euglycaemic clamp pilot study assessing the effects of the glucagon receptor antagonist LY2409021 on 24-hour insulin requirement in patients with type 1 diabetes mellitus. In *American Diabetes Association 73rd Scientific Sessions*. Chicago , IL,

FIGURES

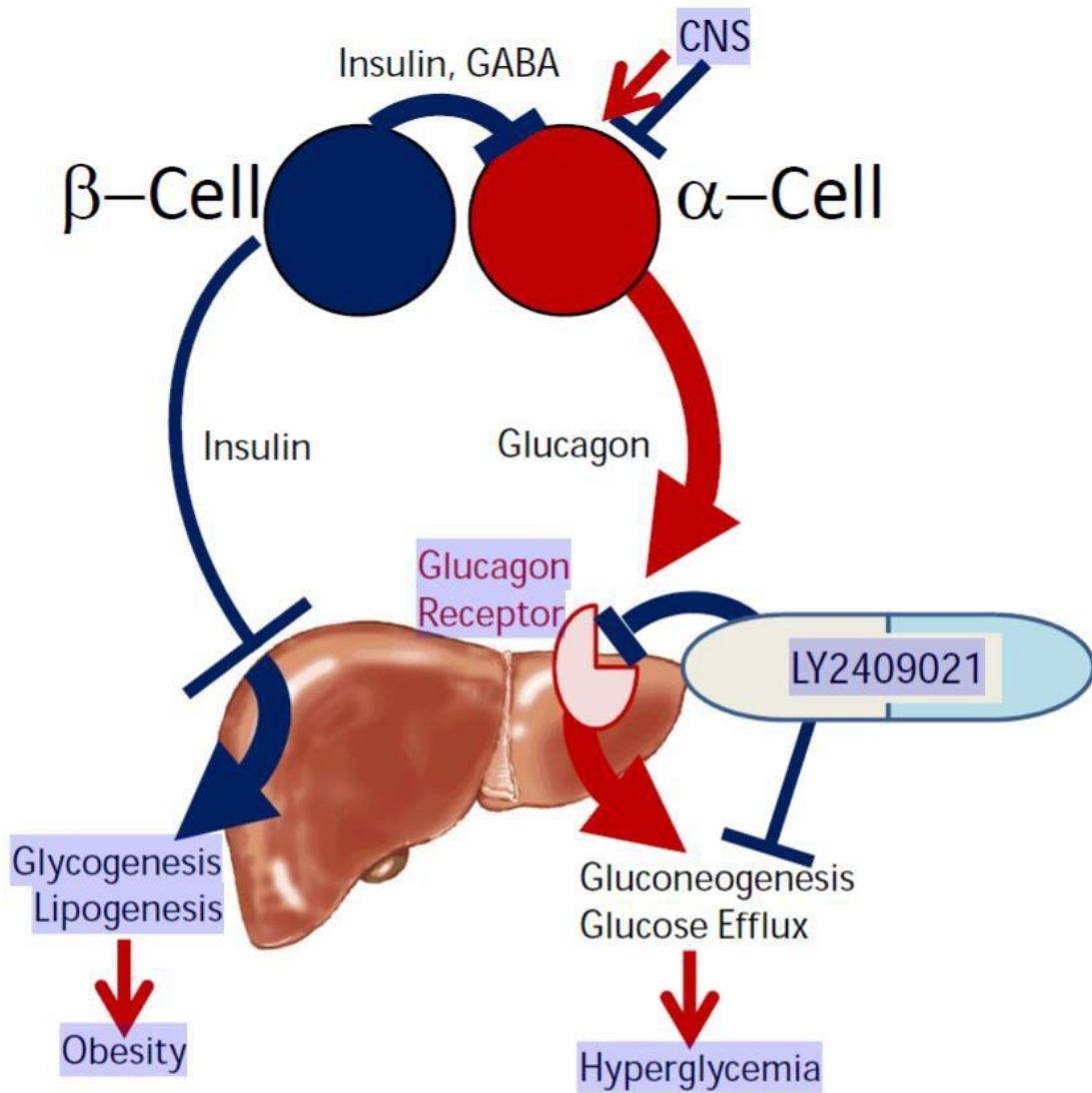


Figure 1. The bihormonal regulation of glucose by insulin and glucagon. Insulin suppresses glucagon secretion while promoting lipid and carbohydrate storage. Glucagon prompts gluconeogenesis and glucose efflux from the liver. LY2409021 decreases serum glucose by preventing glucagon receptor activation and alleviating excess gluconeogenesis.

Chapter 2

Ceramide Accumulation in the Alpha Cell Drives Glucagon Secretion and Hyperglycemia

This is adapted from a publication that is currently in progress

Mackenzie J Pearson¹, Young Lee^{1,2}, Joshua A. Johnson¹, Shihwei Chen¹, Ezekiel Quittner-Strom¹, Ankit X. Sharma¹, Xinxin Yu^{1,2}, Andie C. Dorn¹, Jeffrey G. McDonald², Ruth Gordillo¹, Roger H. Unger^{1,3} and William L. Holland^{1†}

¹Touchstone Diabetes Center, Department of Internal Medicine

² Center for Human Nutrition

The University of Texas Southwestern Medical Center, Dallas, Texas 75390-8549

³Medical Service, Veteran's Administration North Texas Health Care System, Dallas, TX

75216

† Correspondence should be addressed to:

William L. Holland

Touchstone Diabetes Center

Department of Internal Medicine

University of Texas Southwestern Medical Center

5323 Harry Hines Blvd.

Dallas, TX, 75390-8549, USA

Email: William.Holland@UTSouthwestern.edu

Tel: 214-648-2566

Fax: 214-648-8720

Running title: Ceramides Drive Hyperglucagonemia

Pancreatic islets secrete both insulin and glucagon in a tightly juxtaposed manner. Insulin promotes the uptake and storage of carbohydrates and other nutrients in skeletal muscle and fat, while simultaneously repressing both glucagon secretion from pancreatic α -cells and glucose efflux from the liver. The hormone glucagon, which promotes hepatic glycogenolysis and gluconeogenesis, is an underestimated contributor to metabolic disease. Both Type-1 DM and Type-2 DM are associated with hyperglucagonemia and an increased plasma glucagon:insulin ratio¹. Insulin, gamma aminobutyric acid (GABA), and somatostatin signaling in the pancreatic α -cell dampen glucagon production and secretion². Ceramides, bioactive lipids derived from saturated fats, contribute to lipid-induced apoptosis and dysfunction of insulin-producing beta cells³⁻⁵. Although ceramides can antagonize the signaling of insulin and other growth factors in muscle and liver⁶, the consequence of ceramides or other ectopic lipids in pancreatic α -cells is unexplored. Here, I investigate the role of ceramide within the α -cell and uncover a key link between abnormal lipid metabolism that promotes the aberrant glucagon and glucose production associated with diabetes.

The α -cell is an insulin-responsive cell type. After ingestion of glucose, the first-phase spike in insulin is believed to constitute the paracrine signal that suppresses glucagon². The high insulin/low glucagon ratio converts the liver into a glucose-storing organ¹ as opposed to the glucose producing organ needed between meals. If insulin is neutralized in a normal pancreas by perfusing it with insulin anti-serum, marked hypersecretion of glucagon results⁷. Similarly, in elegant studies by the Kulkarni group, α -cells made insulin resistant by insulin receptor ablation *in vitro* or *in vivo* facilitate hyperglucagonemia and hyperglycemia⁸. In T2D, glucagon remains unsuppressed by insulin, even when insulin is given as a bolus with a meal⁹. As such, I hypothesized that this represents a pathophysiology defined by hormonal resistance to insulin and other factors within the α -cell, which prevent suppression of glucagon secretion.

Insulin resistance is a strong risk factor for T2D¹⁰; however, the mechanisms linking impaired insulin action to frank hyperglycemia remain unclear. A leading theory for the mechanism driving peripheral insulin resistance is attributed to ectopic deposition of lipid, resulting in lipid intermediates, such as ceramide or diacylglycerol (DAG)¹¹⁻¹³. Both sphingolipid³ and glycerolipid¹⁴ metabolites are known to accumulate in islets of diabetic rodents. We have shown that islets from diabetes-prone Zucker Diabetic Fatty rats convert fatty acids into ceramide via *de novo* synthesis at a much greater rate than lean littermates^{3,15}. Blocking the committed-step in ceramide biosynthesis, the condensation of palmitoyl-CoA and L-serine (catalyzed by the enzyme serine palmitoyltransferase, SPT) prevents lipotoxic apoptosis in β -cells; α -cells were not evaluated³. Piro and colleagues have ~~recently~~ demonstrated that saturated fatty acids cause insulin resistance of *in vitro* α -cells by reducing activation of insulin's signal transducers¹⁶.

Sphingolipids, such as ceramides and glucosylceramides, are an important class of bioactive lipids that impair insulin signal transduction in muscle, liver, and adipose. The levels of these lipids change as a function of obesity and inflammatory stimuli, and are partially driven by cellular availability of palmitoyl-CoA¹⁷. Aberrant accumulation of sphingolipids has been implicated in a multitude of metabolic processes, including atherosclerosis, insulin resistance, lipotoxic heart failure, β -cell apoptosis and β -cell dysfunction [reviewed in¹²]. In mammals, ceramides are produced *de novo* in each cell type, and these lipids can traffic from tissue to tissue in the serum^{6,18}. Cellular elimination of ceramides is initiated by ceramidase enzymes, with lysosomal acid ceramidase responsible for the bulk of ceramide deacylation into sphingosine and free fatty acid in tissues outside the digestive tract. Tetracycline-dependent overexpression of acid ceramidase allows for the inducible, titratable, tissue-specific degradation of ceramides¹⁹. Here, we overexpress acid ceramidase locally within the mature

α -cell to degrade ceramides from both intracellular and systemic sources in order to explore the influence of ceramides on the regulation of glucagon secretion (**extended data Fig. 1**).

Ceramide Promotes Glucagon Production and Secretion *In Vitro* and *Ex Vivo*

In order to promote ceramide accumulation in cultured α -cells, cultured InR1G9 hamster α -cells were incubated with the saturated fatty acid palmitate (**Fig. 1a**). This drove a 46% increase in total ceramide content (primarily consisting of 16-, 18-, or 20-carbon acyl chains) which was completely blocked by including the SPT inhibitor myriocin. Palmitate drove glucagon transcription (**Fig. 1b**) and glucagon secretion (**Fig. 1c**) only when ceramide synthesis was allowed. When the short chain ceramide analog C2-ceramide is added to InR1G9 cells insulin is unable to suppress the levels of glucagon mRNA being endogenously produced or glucagon secretion into media (**Fig. 1d&e**). Akt (Protein Kinase B), a key mediator in insulin's pleiotropic effects, is phosphorylated following insulin stimulation (**Fig. 1f**). C2-ceramide treatment blunted Akt phosphorylation, indicative of impairments in insulin sensitivity.

Protein phosphatase 2A (PP2A), which removes activating phosphate groups from Akt, has been implicated as a critical mediator of ceramide-induced insulin resistance in other cell types. To investigate the role of PP2A in ceramide-mediated glucagon secretion, InR1G9 cells were treated with the PP2A inhibitor okadaic acid (OkAc) prior to assessing glucagon secretion in the presence of C2-ceramide or Insulin. Okadaic acid blunts ceramide-induced increases in glucagon secretion into the media under basal or insulin stimulated conditions (**Fig. 1e**), suggesting that ceramide relies on PP2A to mediate rapid effects on glucagon secretion. Moreover, okadaic acid enhances insulin-induced suppression of glucagon secretion. Isradapine, an inhibitor of L-type calcium channels also prevents ceramide-induced glucagon secretion, while activation of L-type calcium channels with BayK8644 recapitulates enhanced

glucagon secretion. In culture, ceramide-induced secretion of glucagon is consistent with mechanisms requiring the inhibition of Akt, and alteration of L-type calcium channels.

To assess the effects of C2-ceramide on *bona fide* intact α -cells, we perfused C2-ceramide through the celiac artery while assessing insulin (**Fig. 1g**) and glucagon (**Fig. 1h**) secretion into the portal vein effluent. C2-ceramide enhanced glucagon secretion under conditions mimicking low (2mM) and normal (5 mM) blood glucose. The excess glucagon secretion could not be explained as a secondary effect influenced by the β -cell, as C2-ceramide enhanced insulin secretion under low-glucose conditions. Under conditions mimicking hyperglycemia (20 mM glucose), glucagon secretion remained low and was unchanged by C2-ceramide; by contrast, insulin secretion was almost doubled by the presence of C2-ceramide. Thus, ceramide is sufficient to drive glucagon production in the murine pancreas, unless insulin secretion is sufficiently high.

Acid ceramidase overexpression in the α -cell improves α -cell insulin action in the clamped state.

In order to lower ceramides locally within the α -cell, acid ceramidase transgenic mice engineered under the control of a tetracycline response element (TRE-AC)²⁰ were crossed with reverse tetracycline transactivator mice with expression controlled by the preproglucagon promoter (PPG-rtTA) (**extended data Fig. 2a**)²¹. The resulting PPG-AC mice allowed for a 3.84±0.26 fold increase in acid ceramidase expression within the islet compared to PPG-WT (lacking TRE-AC) littermates after 2 weeks of induction with doxycycline (dox) chow (**extended data Fig. 2b**). Expression of preproglucagon (PPG), glucagon, insulin1, and insulin2 remain unchanged between the two groups. Immunofluorescent microscopy demonstrates that expression of acid ceramidase increases selectively within the α -cell, raising alpha cell acid ceramidase signal to be on par with adjacent β -cell expression (**Fig. 2a**). On a dox-chow diet,

PPG-AC mice and PPG-WT mice display similar glucose tolerance as PPG-WT mice (**extended data Fig. 2c**), but show mildly greater glucose clearance during insulin tolerance tests (**Fig. 2b**). In PPG-AC mice, Acid ceramidase expression did not change in tissues adipose, liver, or hindbrain (**extended data Fig. 2d**).

To assess insulin action on the alpha cell in a physiologic context, hyperinsulinemic-hypoglycemic clamps were performed on lean PPG-AC mice and their wildtype counterparts. In the fasted state, prior to initiating clamps, glucagon is 48% lower in PPG-AC mice than PPG-WT mice (**Fig. 2c**). As expected, achieving hypoglycemia (**Fig. 2d**) in PPG-WT mice drove a strong increase in circulating glucagon concentrations. By contrast, PPG-AC mice showed little increase in glucagon despite achieving the same degree of hypoglycemia. The glucose infusion rate (GIR) required to maintain blood glucose at 41 mg/dL is nearly three times higher in the PPG-AC animals (**Fig. 2d**). Collectively, these data suggest that acid ceramidase overexpression in the alpha cell may blunt glucagon secretion and enhance alpha cell insulin sensitivity.

Acid ceramidase overexpression in the α -cell prevents hyperglycemia in diet-induced obesity

Male PPG-AC and PPG-WT mice were metabolically challenged with a doxycycline-enriched high-fat diet (Dox-HFD) beginning at 8-weeks of age. Body weights were no different between groups at any time following Dox-HFD. After 3 weeks of Dox-HFD, the PPG-AC mice began to display lower random-fed blood glucose compared to PPG-WT mice (**Fig. 3a**). After 8 weeks of Dox-HFD, fasting blood glucose was lower in PPG-AC mice than PPG-WT mice, however, glucose tolerance was not different (**extended data Fig. 3a**). Glucose excursion following a mixed meal was mildly improved in PPG-AC mice compared to PPG-WT mice

(**extended data Fig. 3b**). Overexpression of acid ceramidase enhanced insulin-stimulated clearance of blood glucose during an insulin tolerance test (**Fig. 3b**). This may be due to less counter-regulation by glucagon, as circulating glucagon was 3.2-fold lower in PPG-AC mice than PPG-WT mice (**Fig. 3c**). The neurotransmitter GABA is co-secreted in insulin granules and helps to suppress glucagon secretion. GABA administration decreased glucagon secretion much more effectively in PPG-AC mice than PPG-WT mice suggesting improved GABA sensitivity in the alpha cell (**Fig. 3d**); lowering ceramides may blunt glucagon suppression by multiple endogenous suppressors. Intestinal L-cells, which produce the incretin peptide glucagon-like peptide 1 (GLP-1), also contain proglucagon; however, serum concentrations of active GLP-1 were not different between groups (**extended data Fig. 3c**).

Histologic assessment of H&E stained pancreatic sections suggests that islets are a comparable size between both genotypes with no gross changes in islet morphology (**Fig. 3e**). Immunostaining for insulin and glucagon, demonstrates marked alpha cell hyperplasia in PPG-AC mice, with an unusual abundance of glucagon positive cells in the medulla of the islet (**Fig. 3f**). After 8 weeks of Dox-HFD, ceramide content was significantly lower in PPG-AC islets for the majority of ceramide species (**Fig. 3g**). Neither total diacylglycerol nor 18:2 diacylglycerol, the most potent activator of protein kinase C, differed in abundance between islets of each genotype (**extended data Fig. 3c&d**).

After a 16-week exposure to high-fat diet, PPG-AC mice displayed improvements in glucose tolerance (**Fig. 4a**), however body weights remained similar between both genotypes (**extended data Fig. 4a**). As an assessment of gluconeogenesis, glucose excursion following a pyruvate challenge was definitively lower in PPG-AC mice than PPG-WT mice (**Fig. 4b**). Circulating insulin levels were similar between groups in both the fasted state and following glucose challenge (**Fig. 4c**). Arginine-stimulated insulin secretion (an assessment of readily-secretable insulin) was nearly identical in PPG-AC and PPG-WT mice (**Fig. 4d**). Moreover,

arginine potentially stimulated glucagon secretion to a similar extent in mice of each genotype (**Fig. 4e**).

To assess ceramide content locally within the alpha cell, a tdTomato fluorescent reporter was co-expressed in preproglucagon positive cells. To achieve this, PPG-AC and PPG-rtTA mice were crossed with mice harboring an allele of Cre recombinase encoded behind the control of a tetracycline response element (TRE-Cre) and mice encoding tdTomato with lox-STOP-lox sequence separating it from the ubiquitously expressed ROSA promoter (*Rosa26-loxP-STOP-loxP-tdTomato*). Following a 16-week exposure to Dox-HFD islets were isolated, dispersed, and fluorescence-activated cell sorting was performed to segregate and count Tomato⁺ α -cells and Tomato⁻ cells (consisting predominantly of β -cells). In Tomato⁺ α -cells, PPG-AC expression effectively lowers ceramides of all detected chain lengths (**Fig. 4f**). By contrast, none of the ceramide species measured from Tomato⁻ cells were significantly ($p > 0.11$) altered by expression of acid ceramidase in the neighboring α -cells (**Fig. 4g**). Total ceramide content was reduced in PPG-AC alpha cells compared to PPG-WT alpha cells (**Fig. 4h**). Neither glucosylceramides nor total sphingomyelin content were significantly altered by acid ceramidase overexpression (**extended data Fig. 4b&c**).

Under this chronic HFD-Dox treatment condition, multiple markers of metabolic health improved in non-pancreatic tissues. Notably, hepatic steatosis was diminished as histologically evident by decreased abundance of lipid droplets (**extended data Fig. 4c**), which was further confirmed by biochemical measurement of hepatic triglyceride content (**extended data Fig. 4d**). Although adiposity was comparable between genotypes, adipocyte size was smaller in PPG-AC mice than PPG-WT mice (**extended data Fig. 4e**). Moreover, decreased abundance of crown-like structures and decreased trichrome staining in PPG-AC mice suggest decreased macrophage infiltration and decreased adipose fibrosis, respectively. This might be too much of a distraction from the main message, even though it is buried as supplement.

Acid ceramidase overexpression in the α -cell prevents hyperglycemia in leptin deficient mice

To evaluate the effects of alpha cell ceramide accrual during the onset of frank diabetes, PPG-AC mice were crossed into the leptin-deficient $Lep^{ob/ob}$ background. At 5-weeks of age, blood glucose (**Fig. 5a**) and body weight (**Fig. 5b**) were equivalent in $Lep^{ob/ob}$ PPG-AC and $Lep^{ob/ob}$ PPG-WT mice, and dox-chow diets were initiated. Over a 10-week period, $Lep^{ob/ob}$ PPG-AC mice were completely refractory to hyperglycemia and never displayed blood glucose greater than 164 mg/dL (**Fig. 5a**). However, $Lep^{ob/ob}$ PPG-WT littermates spontaneously developed overt hyperglycemia averaging 340 mg/dL. Body weights remained similar between groups (**Fig. 5b**). Glucose tolerance was markedly better in $Lep^{ob/ob}$ PPG-AC than $Lep^{ob/ob}$ PPG-WT mice (**Fig. 5c**) During pyruvate challenge, $Lep^{ob/ob}$ PPG-AC mice showed profound differences in circulating glucose, suggesting better suppression of gluconeogenesis (**Fig. 5d**). These changes corresponded with changes in circulating glucagon, which was 4.3-fold higher in serum from 10-week old diabetic $Lep^{ob/ob}$ PPG-WT than the same mice at 5-weeks age; glucagon remained normal in $Lep^{ob/ob}$ PPG-AC mice (**Fig. 5e**).

In $Lep^{ob/ob}$ PPG-AC mice, insulin tolerance tests suggested improved lowering of blood glucose (**Fig. 5f**), however, circulating insulin remained similar between groups (**extended data Fig. 5a**). To assess whole-body insulin sensitivity, we performed hyperinsulinemic-euglycemic clamps, which revealed a 4.2-fold increase in the glucose infusion rate required to maintain euglycemia in $Lep^{ob/ob}$ PPG-AC (**Fig. 5g**). This perceived improvement in insulin sensitivity could not be explained by the minor differences in circulating glucose during the clamped state (210.5 \pm 18.7 mg/dL for $Lep^{ob/ob}$ PPG-WT; 180.7 \pm 5.3 mg/dL for $Lep^{ob/ob}$ PPG-AC), or circulating insulin, but may be driven by the lower abundance of circulating glucagon in $Lep^{ob/ob}$ PPG-AC

mice (**extended data Fig. 5b**). The liver accounted for the majority of the change in “insulin sensitivity”, as endogenous glucose production was diminished in Lep^{ob/ob}PPG-AC mice (**Fig 5h**). Further analysis of liver from these mice demonstrated enhanced suppression of gluconeogenic genes: glucose 6-phosphatase (G6Pase), phosphoenolpyruvate carboxykinase (PECK), and Foxo1 (**Fig. 5i**). Phosphorylation of carbohydrate response-element binding protein (Creb), a central regulator of glucagon action and PEPCK expression, was greatly diminished in Lep^{ob/ob}PPG-AC mice as compared to their Lep^{ob/ob}PPG-WT littermates (**Fig. 5j**).

Examination of pancreatic sections of Lep^{ob/ob}PPG-AC mice suggest that total pancreatic islet size was similar on average, but showed signs of alpha cell hyperplasia with abnormal distribution of alpha cells in the medulla of the islet (**Fig. 5k and extended data Fig. 5c**). Total insulin and glucagon protein, determined after acid-ethanol extraction, indicated decreased insulin content and a trend toward decreased glucagon content in pancreas of Lep^{ob/ob}PPG-AC as compared with Lep^{ob/ob}PPG-WT controls (**extended data Fig. 5d&e**). Arginine-induced secretion of insulin and glucagon, suggest that expression of acid ceramidase did not alter the secretory capacity for glucagon or insulin (**extended data Fig. 5f&g**). To directly evaluate the secretion of insulin and glucagon we performed pancreatic perfusions through the celiac artery (**Fig. 5l**). During perfusion of 6 mM glucose (normoglycemia) or 2 mM glucose (hypoglycemia) glucagon levels remained lower in Lep^{ob/ob}PPG-AC mice, and glucagon failed to increase as glucose levels dropped. Insulin secretion in Lep^{ob/ob}PPG-AC mice was not different during perfusion of 6 mM glucose and 20 mM glucose (hyperglycemia), but insulin secretion during 2 mM glucose declined more slowly as compared to Lep^{ob/ob}PPG-WT mice. These perfusion data suggest that acid ceramidase expression in the alpha cell blunts glucagon secretion, but does not enhance insulin secretion.

In the leptin-deficient background, alpha cell expression of acid ceramidase improves multiple markers of metabolic health improved in non-pancreatic tissues. Less hepatic steatosis

was visible in H&E-stained liver sections, which was enzymatically confirmed (**extended data Fig. 5h&i**). Although adiposity was comparable between genotypes, crown-like structures were less abundant in adipose from Lep^{ob/ob}PPG-AC mice than Lep^{ob/ob}PPG-WT mice (**extended data Fig. 5j**). Again, this might be too much of a distraction from the main message, even though it is buried as supplement.

Acid ceramidase overexpression in the alpha cell reverses hyperglycemia in obese diabetic mice

Given the inducible nature of the PPG-AC mice, we next assessed if induction of the acid ceramidase transgene could reverse hyperglycemia in diabetic mice. While maintained on a doxycycline-free high fat diet, multiple doses of streptozotocin (STZ, a potent inducer of beta cell death) administration promoted hyperglycemia (**Fig. 6a**). Before providing dox in the diet, PPG-AC and PPG-WT mice developed similar hyperglycemia with similar body weights (**extended data Fig. 6a**). After switching mice to dox-HFD, PPG-AC mice markedly improved fed blood glucose within 48 hours, and maintained their blood glucose for the remainder of dox-HFD treatment. Dox-HFD had no effect on blood glucose of PPG-WT mice. Oral glucose tolerance (**Fig. 6b**) and pyruvate tolerance (**Fig. 6c**) revealed lower blood glucose in PPG-AC mice throughout each test.

As noted in figure 4, long-term administration of HFD prompted mild diabetes in PPG-WT mice (**Fig. 4b**). Following a 7-week exposure to dox-free HFD, PPG-AC (192.2 mg/dL) and PPG-WT (207.0 mg/dL) mice developed similar hyperglycemia prior to the administration of doxycycline (**Fig. 6d**). After 1 week of dox-HFD, blood glucose substantially dropped in PPG-AC mice and continued to drop for two consecutive weeks; PPG-WT mice remained hyperglycemic. Body weights remained similar between genotypes as both groups continued to

gain weight (**extended data Fig. 6b**). Prior to doxycycline, circulating glucagon levels were not different between genotypes (**Fig. 6e**). After dox-HFD, glucagon continued to rise in PPG-WT mice, but dropped in PPG-AC mice. Glucose excursion during pyruvate tolerance tests was blunted in PPG-AC mice, as compared to PPG-WT mice (**Fig. 6f**).

To assess whether glycemia could be normalized after the onset of diabetes in a well-validated genetic model, Lep^{ob/ob} mice were aged to 11-weeks, producing equivalent hyperglycemia in Lep^{ob/ob}PPG-AC (305 mg/dL) and Lep^{ob/ob}PPG-WT mice (288.2 mg/dL) prior to doxycycline exposure. After doxycycline, blood glucose in Lep^{ob/ob}PPG-AC mice continued to decline for four consecutive weeks (**Fig. 6g**). Glucagon levels were unchanged for Lep^{ob/ob}PPG-AC mice pre and post dox diet, levels in the wildtype continued to rise (**Fig. 6h**). At 14-weeks of age, challenges to both pyruvate and insulin are improved in Lep^{ob/ob}PPG-AC mice (**Fig. 6i&j**). Thus, targeting the ceramide degradation in preproglucagon positive cells can improve glucose homeostasis in multiple models of diabetes.

Here, we elucidate a previously overlooked role for ceramide in the pathophysiology of glucagon hypersecretion. Ceramide is sufficient to promote glucagon secretion, and necessary for the hypersecretion of glucagon in response to chronic HFD or leptin-deficient diabetes. The importance for ceramide in the alpha cell fails to surface in mice with diet-induced insulin resistance, but rather, emerges during the onset of frank diabetes. As such, this suggests that ceramide accumulation within the alpha cell may play a causal role in promoting the aberrant secretion of glucagon. In effect, the ceramide-induced impairments in alpha cell response to insulin, GABA or other suppressors may be a causal link between insulin resistance and hyperglycemia.

Strategies for inhibiting ceramide biosynthesis or promoting ceramide degradation are currently being pursued as potential therapies for the treatment or prevention of type-2 diabetes.

These data suggest the importance of an unforeseen target, the alpha cell, which must be reached by future compounds in order to provide full antidiabetic efficacy. Notably, acid ceramidase overexpression in the hepatocyte or the adipocyte fails to lower blood glucose or improve glucose tolerance in the Lep^{ob/ob} background²², both of which are improved in Lep^{ob/ob}PPG-AC mice. The alpha cell hyperplasia in these models is notable, and consistent with observed effects in glucagon receptor knockout mice^{23,24}. A driving force behind alpha cell hyperplasia that occurs when glucagon receptors are inhibited, and presumably here, is the feedback of glutamine and other amino acids (which would have been used for gluconeogenesis).

While these studies suggest an important role for ceramides, they do not rule out other lipids such as diacylglycerol or phosphatidic acid, as similar effectors of glucagon production via insulin desensitizing actions. Due to the limited abundance of the murine alpha cell in wildtype mice (25,000 cells), targeted lipidomics could not provide sufficient sensitivity to assess other sphingolipid intermediates in detail. Moreover, the relative paucity of phosphatidic acid and isobaric overlaps of this lipid, prevent our current methods from assessing the potential contributions of this glycerolipid to our phenotype.

References

1. Unger, R.H. & Cherrington, A.D. Glucagonocentric restructuring of diabetes: a pathophysiologic and therapeutic makeover. *The Journal of clinical investigation* **122**, 4-12 (2012).
2. Unger, R.H. & Orci, L. Paracrinology of islets and the paracrinopathy of diabetes. *Proceedings of the National Academy of Sciences of the United States of America* **107**, 16009-16012 (2010).
3. Shimabukuro, M., *et al.* Lipoapoptosis in beta-cells of obese prediabetic fa/fa rats. Role of serine palmitoyltransferase overexpression. *The Journal of biological chemistry* **273**, 32487-32490 (1998).
4. Kelpke, C.L., *et al.* Palmitate inhibition of insulin gene expression is mediated at the transcriptional level via ceramide synthesis. *The Journal of biological chemistry* **278**, 30015-30021 (2003).
5. Hagman, D.K., Hays, L.B., Parazzoli, S.D. & Poitout, V. Palmitate inhibits insulin gene expression by altering PDX-1 nuclear localization and reducing MafA expression in isolated rat islets of Langerhans. *The Journal of biological chemistry* **280**, 32413-32418 (2005).
6. Holland, W.L., *et al.* Inhibition of ceramide synthesis ameliorates glucocorticoid-, saturated-fat-, and obesity-induced insulin resistance. *Cell Metab* **5**, 167-179 (2007).
7. Maruyama, H., Hisatomi, A., Orci, L., Grodsky, G.M. & Unger, R.H. Insulin within islets is a physiologic glucagon release inhibitor. *The Journal of clinical investigation* **74**, 2296-2299 (1984).
8. Kawamori, D., *et al.* Insulin signaling in alpha cells modulates glucagon secretion in vivo. *Cell Metab* **9**, 350-361 (2009).
9. Raskin, P. & Unger, R.H. Glucagon and diabetes. *The Medical clinics of North America* **62**, 713-722 (1978).
10. DeFronzo, R.A., *et al.* Type 2 diabetes mellitus. *Nature reviews. Disease primers* **1**, 15019 (2015).
11. Summers, S.A., Lipfert, L. & Birnbaum, M.J. Polyoma middle T antigen activates the Ser/Thr kinase Akt in a PI3-kinase-dependent manner. *Biochemical and biophysical research communications* **246**, 76-81 (1998).
12. Holland, W.L. & Summers, S.A. Sphingolipids, insulin resistance, and metabolic disease: new insights from in vivo manipulation of sphingolipid metabolism. *Endocr Rev* **29**, 381-402 (2008).
13. Savage, D.B., Petersen, K.F. & Shulman, G.I. Disordered lipid metabolism and the pathogenesis of insulin resistance. *Physiol Rev* **87**, 507-520 (2007).
14. Delghingaro-Augusto, V., *et al.* Islet beta cell failure in the 60% pancreatectomised obese hyperlipidaemic Zucker fatty rat: severe dysfunction with altered glycerolipid metabolism without steatosis or a falling beta cell mass. *Diabetologia* **52**, 1122-1132 (2009).
15. Unger, R.H., Scherer, P.E. & Holland, W.L. Dichotomous roles of leptin and adiponectin as enforcers against lipotoxicity during feast and famine. *Molecular biology of the cell* **24**, 3011-3015 (2013).
16. Piro, S., *et al.* Palmitate affects insulin receptor phosphorylation and intracellular insulin signal in a pancreatic alpha-cell line. *Endocrinology* **151**, 4197-4206 (2010).
17. Merrill, A.H., Jr. De novo sphingolipid biosynthesis: a necessary, but dangerous, pathway. *The Journal of biological chemistry* **277**, 25843-25846. (2002).
18. Watt, M.J., *et al.* Regulation of plasma ceramide levels with fatty acid oversupply: evidence that the liver detects and secretes de novo synthesised ceramide. *Diabetologia* **55**, 2741-2746 (2012).
19. Chavez, J.A., Holland, W.L., Bar, J., Sandhoff, K. & Summers, S.A. Acid ceramidase overexpression prevents the inhibitory effects of saturated fatty acids on insulin signaling. *The Journal of biological chemistry* **280**, 20148-20153 (2005).

20. Xia, J.Y., *et al.* Targeted Induction of Ceramide Degradation Leads to Improved Systemic Metabolism and Reduced Hepatic Steatosis. *Cell Metab* **22**, 266-278 (2015).
21. Kusminski, C.M., *et al.* MitoNEET-Parkin Effects in Pancreatic alpha- and beta-Cells, Cellular Survival, and Intra-islet Cross Talk. *Diabetes* **65**, 1534-1555 (2016).
22. Holland, W.L., Xia, J.Y., Johnson, J.A., Sun, K., Pearson, M.J., Sharma, A.X., Quittner-Strom, E., Tippetts, T.S., Gordillo, R., Scherer, P.E. Inducible overexpression of adiponectin receptors highlight the roles of adiponectin-induced ceramidase signaling in lipid and glucose homeostasis. *Molecular Metabolism* **6**, 1-9 (2017).
23. Gelling, R.W., *et al.* Lower blood glucose, hyperglucagonemia, and pancreatic alpha cell hyperplasia in glucagon receptor knockout mice. *Proceedings of the National Academy of Sciences of the United States of America* **100**, 1438-1443 (2003).
24. Longuet, C., *et al.* Liver-specific disruption of the murine glucagon receptor produces alpha-cell hyperplasia: evidence for a circulating alpha-cell growth factor. *Diabetes* **62**, 1196-1205 (2013).

Online Only Methods

Methods and Materials

Animals

All animal experimental protocols were approved by the Institutional Animal Care and Use Committee of University of Texas Southwestern Medical Center at Dallas. All overexpression experiments were performed in a pure C57/Bl6 background. All experiments were conducted using littermate-controlled male mice, with the exception of Lep^{ob/ob} studies which used equivalent numbers of male and female Lep^{ob/ob} mice in each cohort. Preproglucagon (PPG)-rtTA mice were previously generated containing the 1.7-kb PPG promoter [CK]. This mouse was subsequently crossed to the TRE-AC transgenic mice previously described [JX]. All Dox-chow diet (600 mg/kg Dox) or HFD-Dox (600 mg/kg Dox) experiments were performed with identical diets given to control and transgenic littermates. High fat diets (60% fat by caloric content) were compounded with doxycycline and sterilized (Bioserv). To achieve diabetes in high-fat fed mice, animals were fasted for 6 hrs and subjected to injection of STZ (65 mg/kg, IP) once weekly for 5 weeks during weeks 3-8 after starting high fat diet ([Ye et al., 2014](#)).

Systemic tests

For oral glucose tolerance tests, mice were fasted for 4 hours prior to administration of glucose (2.5 g/kg body-weight by gastric gavage). Glucose levels were measured by glucometer (Bayer Contour) and plasma was collected before glucose and 15 minutes after glucose administration. Mice did not have access to food throughout the experiment. Pyruvate was administered 1g/kg body weight by intraperitoneal injection following overnight removal of high fat diet or 4-hour removal of chow diet from Lep^{ob/ob}. For the arginine tolerance test, HFD mice were fasted overnight (12–16 h) and Lep^{ob/ob} mice were fasted for 4 hours before intraperitoneal injection of L-arginine 1 g/kg body weight. Oral gavage of meal (10ul/g of Ensure) was given after a 4-

hour fast and blood glucose was monitored. Insulin tolerance tests were initiated by intraperitoneal injection of 0.75 U/kg (lean and HFDrecombinant human insulin (humalin-R, Lilly)

Plasma Parameters

For glucagon measurement plasma was collected with aprotinin, and glucagon levels were measured by using an ELISA kit (Mercodia Inc., Winston-Salem, NC). Insulin levels were measured using commercial ELISA kits (Crystal Chem).

Quantitative Real-Time PCR

Tissues were excised from mice and snap-frozen in liquid nitrogen. Total RNA was isolated following tissue homogenization in Trizol (Invitrogen, Carlsbad, CA) using a TissueLyser (MagNA Lyser, Roche), then isolated using an RNeasy RNA extraction kit (Qiagen). The quality and quantity of the RNA was determined by absorbance at 260/280 nm. cDNA was prepared by reverse transcribing 1 ug of RNA with an iScript cDNA Synthesis Kit (BioRad). Results were calculated using the threshold cycle method (38), with β -actin or GAPDH used for normalization.

Hyperinsulinemic-clamps

Hyperinsulinemic-euglycemic clamps were performed on conscious, unrestrained Lepo^{ob/ob} mice as previously described (19, 37). Hyperinsulinemic-hypoglycemic clamps were performed as previously described⁸. For both studies hyperinsulinemia was initiated by primed-continuous infusion of insulin (10 mU/kg/min).

Pancreatic Perfusions and Glucagon Secretion assays

Mouse pancreata were perfused with buffers containing either 2.7 mmol/L or 16.7 mmol/L glucose. All buffers before reaching the celiac artery were maintained at 37°C. Perfusates were then collected into aprotinin-containing tubes at 1-min intervals for 25 min into. Insulin and

glucagon levels were measured in perfusates with an insulin assay kit (Cisbio). Glucagon secretion into serum-free, phenol-free RPMI was assessed from InR1G9 cells for 30 minutes after treatment with porcine insulin (sigma, 1 uM), C2-ceramide (Millipore 50 uM, 20 minutes prior to insulin), okadaic acid (Millipore, 500 nM, 10 minutes prior to ceramide), isridapine (sigma, x n, 10 minutes prior to ceramide), BayK (Cayman, x nM, 10 minutes prior to ceramide).

InR1G9 cells were treated with and without 500uM palmitate for 18 hours with and without 5uM myriocin. Ceramides were measured by shotgun lipidomics (n=3 each group). b. InR1G9 cells were treated with and without 500uM palmitate with and without 5uM myriocin. Glucagon mRNA levels are reported normalized to GAPDH (n=3 each group). c. InR1G9 treated cells with and without C2 ceramide and palmitate. Glucagon secretion is reported as a percent of control. (n= 3 each group) d. InR1G9 cells were treated with and without C2 ceramide for 30 minutes. Glucagon mRNA levels were normalized to GAPDH (n=3). e. Okadaic acid was added to InR1G9 cells. Glucagon secretion is reported as a percent of control. f. InR1G9 cells were treated with and without C2 ceramide and with and without 250nM insulin. Cells were collected with protease inhibitors and p-AKT and AKT levels were evaluated using a western blot. g and h. Pancreatic perfusions were performed on PPG-AC and WT mice. Area under the curve measurements are reported for each glucose dose perfused. Insulin and glucagon levels were measured on collected perfusate.

Isolation of TdTomato-Labeled α -Cells by FACS Sorting

After islet isolation, islets (mixed sizes) were handpicked and added to a tube containing 500 μ L enzyme-free cell dissociation solution (Millipore). Islets were allowed to dissociate in a 37°C water bath for 5–7 min before gently pipetting up and down until no visual clumps were observed. This procedure was repeated once. A small aliquot of islet suspension was examined under a light microscope to confirm the presence of a dispersed cell suspension. Cells were

immediately centrifuged (4°C at 500g for 5 min) to remove the supernatant and then resuspended in 500 µL cold sample application buffer (114 mmol/L NaCl, 4.7 mmol/L KCl, 1.2 mmol/L KH₂PO₄, 1.16 mmol/L MgSO₄, 20 mmol/L HEPES, and 2.5 mmol/L CaCl₂; pH 7.3) containing 5 mmol/L glucose and 1% FBS. This procedure was repeated once. The final cell pellets were diluted to 0.5–1 × 10⁶ cells/mL for FACS sorting. Cells were sorted by a BD FACSAria with an argon laser beam tuned to 532 nm at 50-mW output with a 610 ± 10 nm emission filter. C57/BL6 cells were used as the control and to set the sorting parameters. Dispersed cells were sorted at a rate of 1,000 event/s by using normal recovery mode with the temperature setting at 4°C.

Histology and immunofluorescence (IF)

Tissues were excised and fixed in 10% PBS buffered formalin for 24 h. Following paraffin embedding and sectioning (5 µm), tissues were stained with H&E or a Masson's trichrome stain. For IF, paraffin-embedded sections were stained using monoclonal antibodies to Mac2 (1:500, CL8942AP, CEDARLANE Laboratories USA Inc.), Insulin (1:500, A0564, DAKO Products), Glucagon (1:250, ab10988, Abcam), and ASAH1 (1:50, ab74469, Abcam).

Immunoblotting

Frozen tissue was homogenized in TNET buffer (50 mM Tris-HCl, pH 7.6, 150 mM NaCl, 5 mM EDTA, phosphatase inhibitors (Sigma-Aldrich) and protease inhibitors (Roche) and then centrifuged to remove any adipose layer present. After the addition of Triton X-100 (final concentration of 1%), protein concentrations were determined using a bicinchoninic acid assay (BCA) kit (Pierce). Proteins were resolved on 4–20% TGX gel (Bio-Rad) then transferred to nitrocellulose membranes (Protran). pAkt (Ser473, 4060) and total Akt (2920) (Cell Signaling Technology, Inc.) were used (1:1,000) pCreb

and total Creb for insulin signaling studies. Primary antibodies were detected using secondary IgG labeled with infrared dyes emitting at 700 nm (926-32220) or 800 nm (926-32211) (both at 1:5,000 dilutions) (Li-Cor Bioscience) and then visualized on a Li-Cor Odyssey infrared scanner (Li-Cor Bioscience). The scanned data were analyzed and quantitated using Odyssey Version 2.1 software (Li-Cor Bioscience).

Lipid Quantification

Sample Preparation. Flash frozen cell pellets (2x10⁶ cells per sample) in a borosilicate glass tube were quenched with 2.0 mL of organic extraction solvent (isopropanol: ethyl acetate, 15:85; vol:vol). Immediately afterwards, 20 µL of internal standard solution was added (Avanti Polar Lipids, AL Ceramide/Sphingoid Internal Standard Mixture II diluted 1:10 in ethanol). The mixture was vortexed and sonicated in ultrasonic bath during 10 minutes at 40 °C. Then the samples were allowed to reach room temperature and 2 mL of HPLC water was added. Two-phase liquid extraction was performed, the upper phase was transferred to a new tube and the pellet was re-extracted. Supernatants were combined and evaporated under nitrogen. The dried residue was reconstituted in 2.0 mL of Folch solution, 400 µL were transferred to a new tube and were reserved for organic phosphate determination, 300 µL were transferred to a new tube and were reserved for infusion based LC-MS analysis, the remaining volume was reserved for targeted LC/MS/MS sphingolipid analysis. The different organic fractions were dried under nitrogen and stored at -80°C until analysis.

Sphingolipid Analysis. Sphingolipids levels were quantitated using LC/MS/MS methodology using a Nexera X2 UHPLC system coupled to a Shimadzu LCMS-8050 triple quadrupole mass spectrometer operating the Dual Ion Source in Electrospray positive mode.^{1,2} Dried lipid extracts were reconstituted in 200 µL of HPLC solvent (methanol/ formic acid 99:1; vol:vol containing 5 mM ammonium formate) for LC-MS/MS analysis. Lipid separation was achieved on

a 2.1 (i.d.) x 150 mm Kinetex C8, 2.6 micron core-shell particle (Phenomenex, Torrance, CA) column.

Sphingolipids species were identified based on exact mass and fragmentation patterns, and verified by lipid standards. The concentration of each metabolite was determined according to calibration curves using peak-area ratio of analyte vs. corresponding internal standard.

Calibration curves were generated using serial dilutions of each target analyte. Sphingolipid true standards were purchased from Avanti Polar Lipids (Alabaster, AL).

Total Phosphorous Determination. Total phosphorous content in the organic extracts was determined as described by Chen et al., and Fiske and Subbarow.^{3,4}

Statistics

The results are shown as mean±SEM. All statistical analysis was performed in SigmaStat 2.03 (SysStat Software, Point Richmond, CA). Differences between the two groups over time (indicated in the relevant figure legends) were determined by a two-way analysis of variance for repeated measures. For comparisons between two independent groups, a Student's t test was used. Significance was accepted at $P < 0.05$.

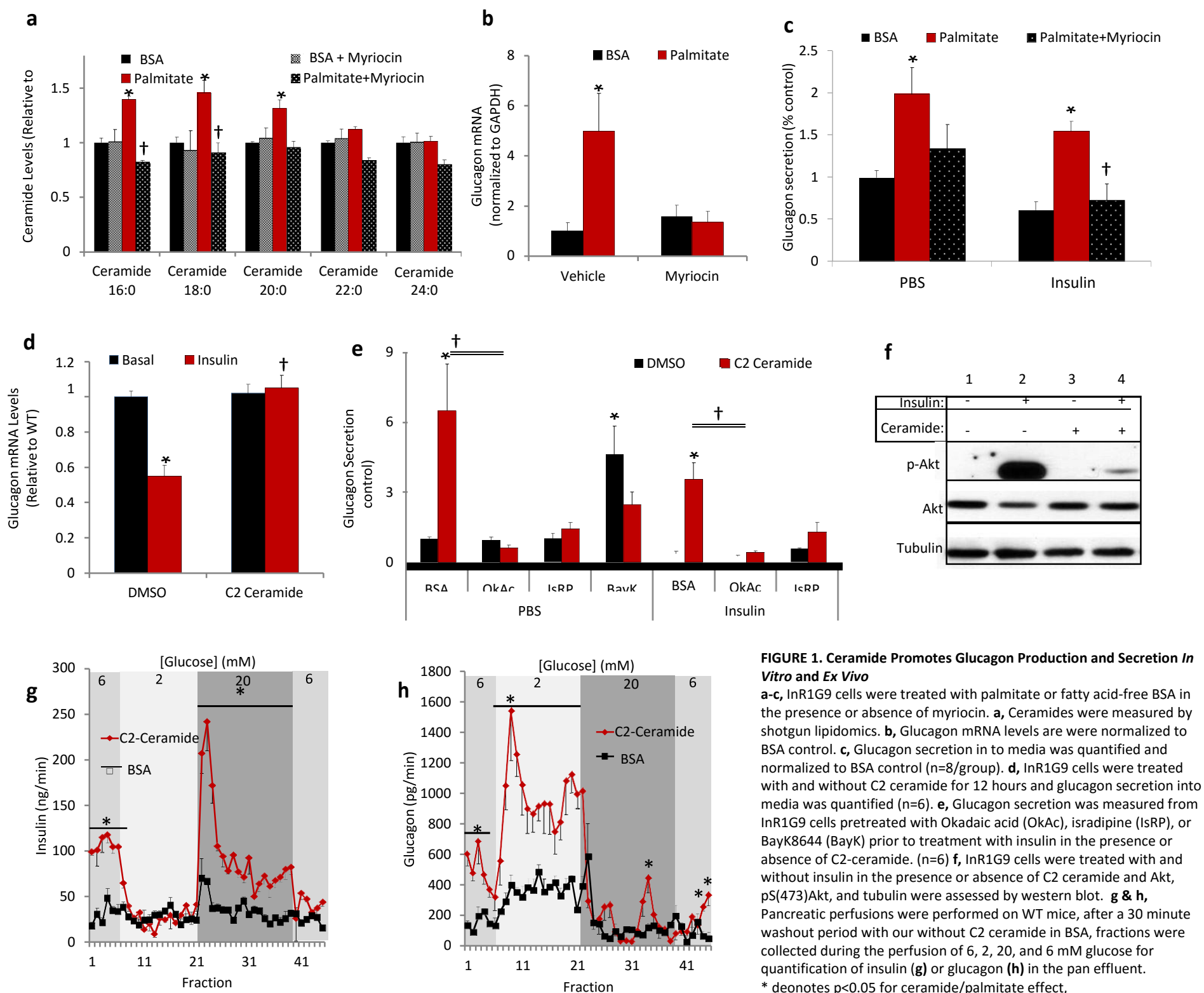
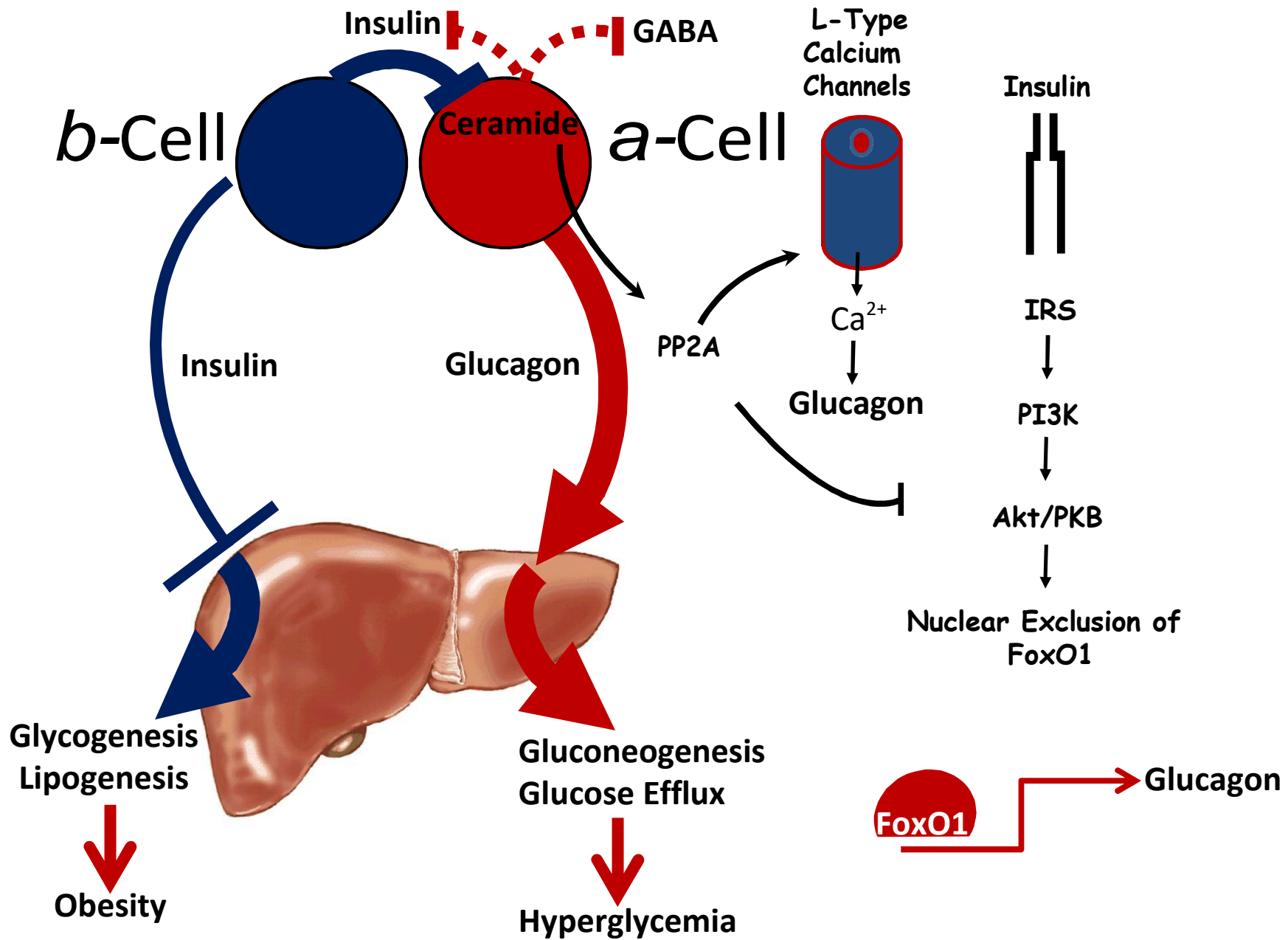


FIGURE 1. Ceramide Promotes Glucagon Production and Secretion *In Vitro* and *Ex Vivo*

a-c, InR1G9 cells were treated with palmitate or fatty acid-free BSA in the presence or absence of myriocin. **a**, Ceramides were measured by shotgun lipidomics. **b**, Glucagon mRNA levels were normalized to BSA control. **c**, Glucagon secretion in to media was quantified and normalized to BSA control (n=8/group). **d**, InR1G9 cells were treated with and without C2 ceramide for 12 hours and glucagon secretion into media was quantified (n=6). **e**, Glucagon secretion was measured from InR1G9 cells pretreated with Okadaic acid (OkAc), isradipine (IsRP), or BayK8644 (BayK) prior to treatment with insulin in the presence or absence of C2-ceramide. (n=6) **f**, InR1G9 cells were treated with and without insulin in the presence or absence of C2 ceramide and Akt, pS(473)Akt, and tubulin were assessed by western blot. **g & h**, Pancreatic perfusions were performed on WT mice, after a 30 minute washout period with or without C2 ceramide in BSA, fractions were collected during the perfusion of 6, 2, 20, and 6 mM glucose for quantification of insulin (**g**) or glucagon (**h**) in the pan effluent. * denotes p<0.05 for ceramide/palmitate effect, † denotes p<0.05 for effect of inhibitor. n=4, unless indicated



Extended Data Figure 1. Schematic of ceramide-induced signaling perturbations in the α -cell. Ceramide promotes glucagon secretion via mechanisms that require PP2A and L-type calcium channels. Ceramide blocks glucagon expression via disruption of Akt signaling to FoxO1. Disrupting ceramide accumulation in the α -cell restores glucagon suppression by insulin and GABA.

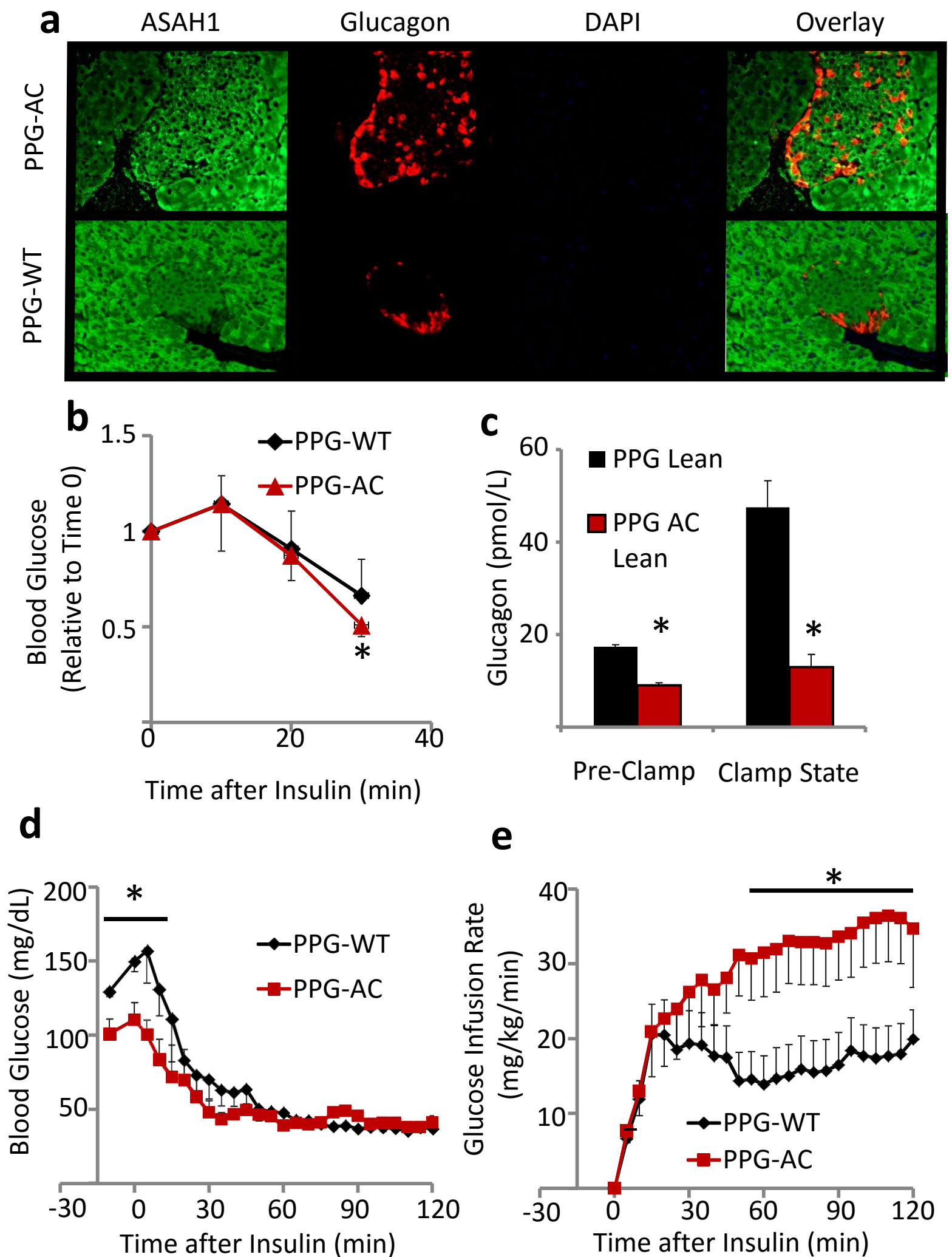
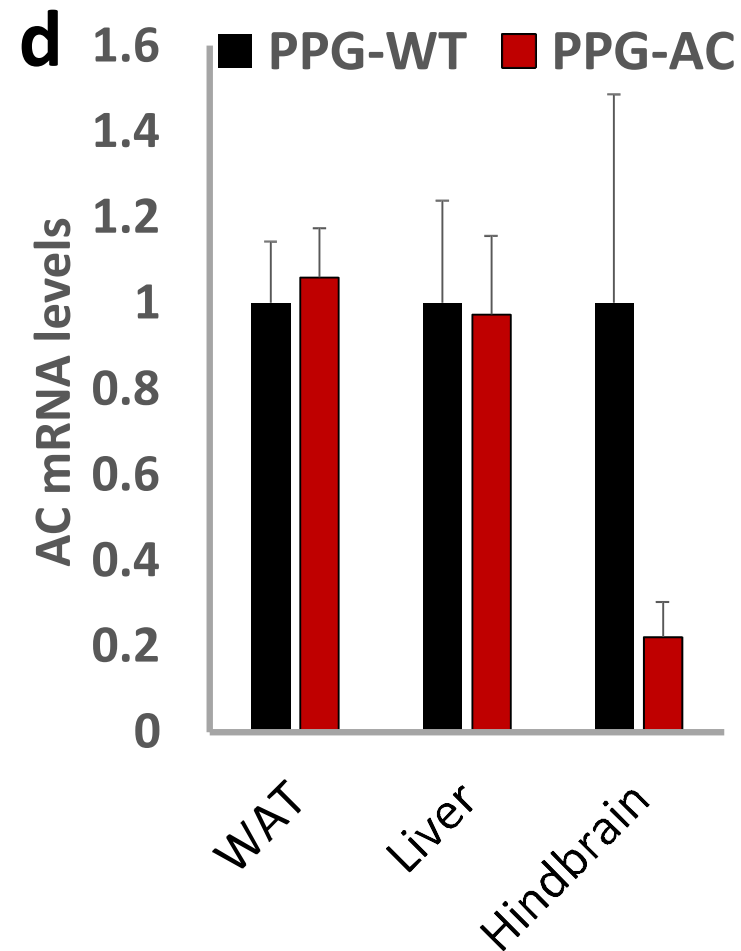
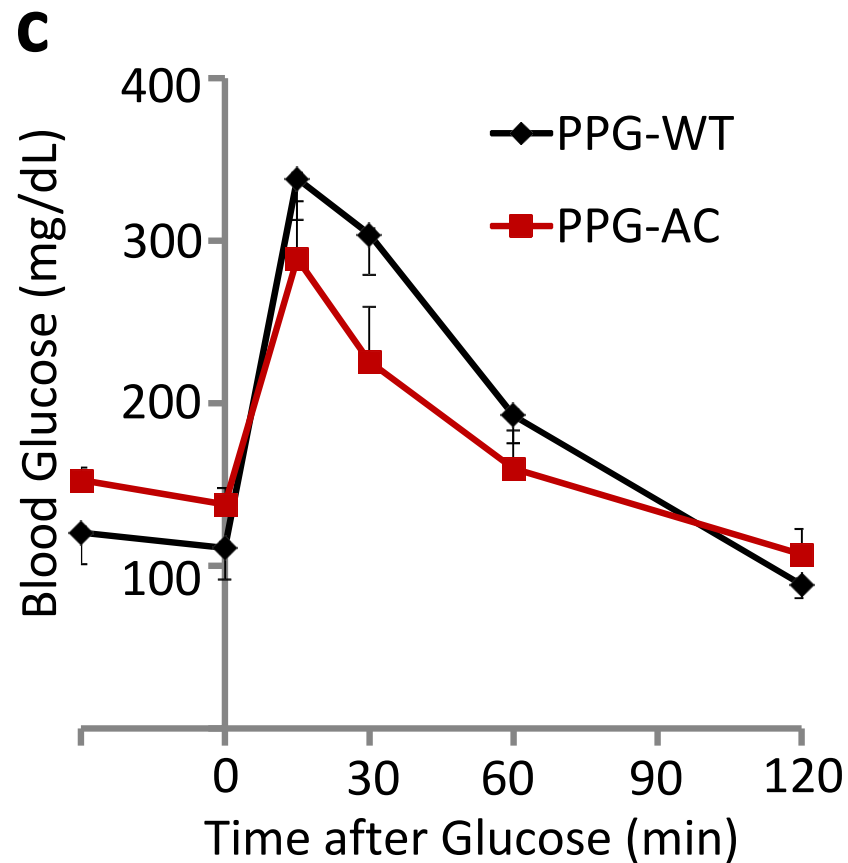
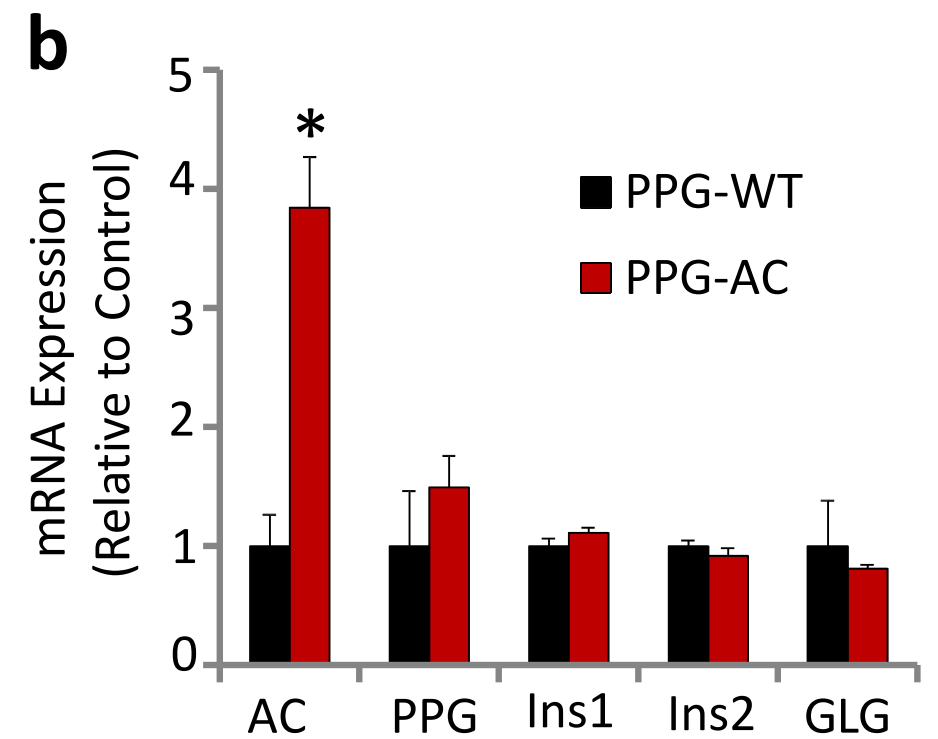
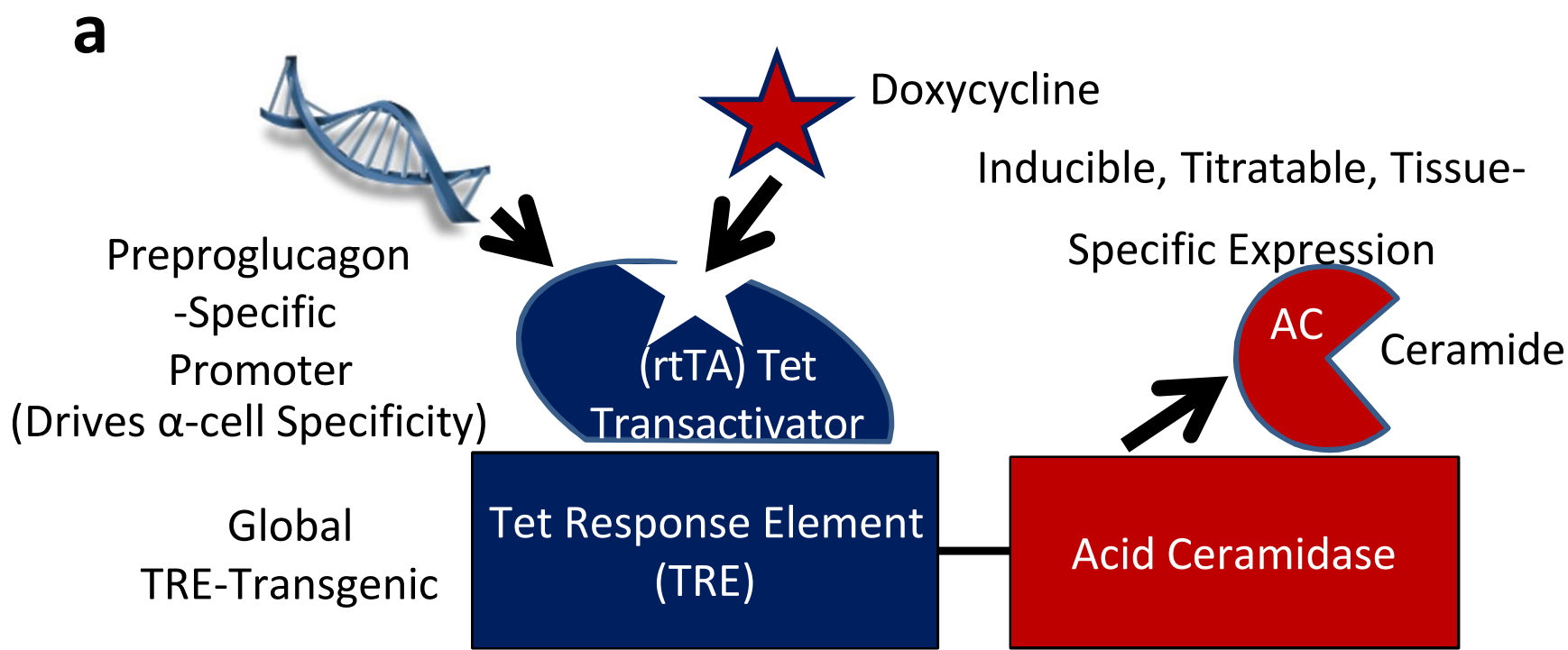


FIGURE 2. Acid ceramidase overexpression in the α -cell improves α -cell insulin action in lean mice.

a, Acid ceramidase (green), glucagon (red), and DAPI (blue) immunofluorescence staining of PPG-AC and WT mice. **b**, insulin tolerance tests. **c-e** hyperinsulinemic-hypoglycemic clamps **c**, Glucagon levels during the fasted (pre-clamp) and clamped state. **d**, Blood glucose of PPG-AC and WT lean mice during clamp. **e**, Glucose infusion rates during clamps. (n=6/group) * denotes $p < 0.05$



EXTENDED DATA FIGURE 2. a, Schematic of the mouse model. Preproglucagon (PPG) -rtTA specific promoter drives alpha-cell specificity. This Tet-transactivator binds to the tet response element upstream of acid ceramidase (tre-AC) to drive overexpression when doxycycline is present. **b**, mRNA expression from isolated islets. **c**, blood glucose levels during an oral glucose tolerance test. **d**, Analysis of mRNA expression from liver, gonadal white adipose tissue, hindbrain, and ileum. $n=6/\text{group}$, $*p<0.05$

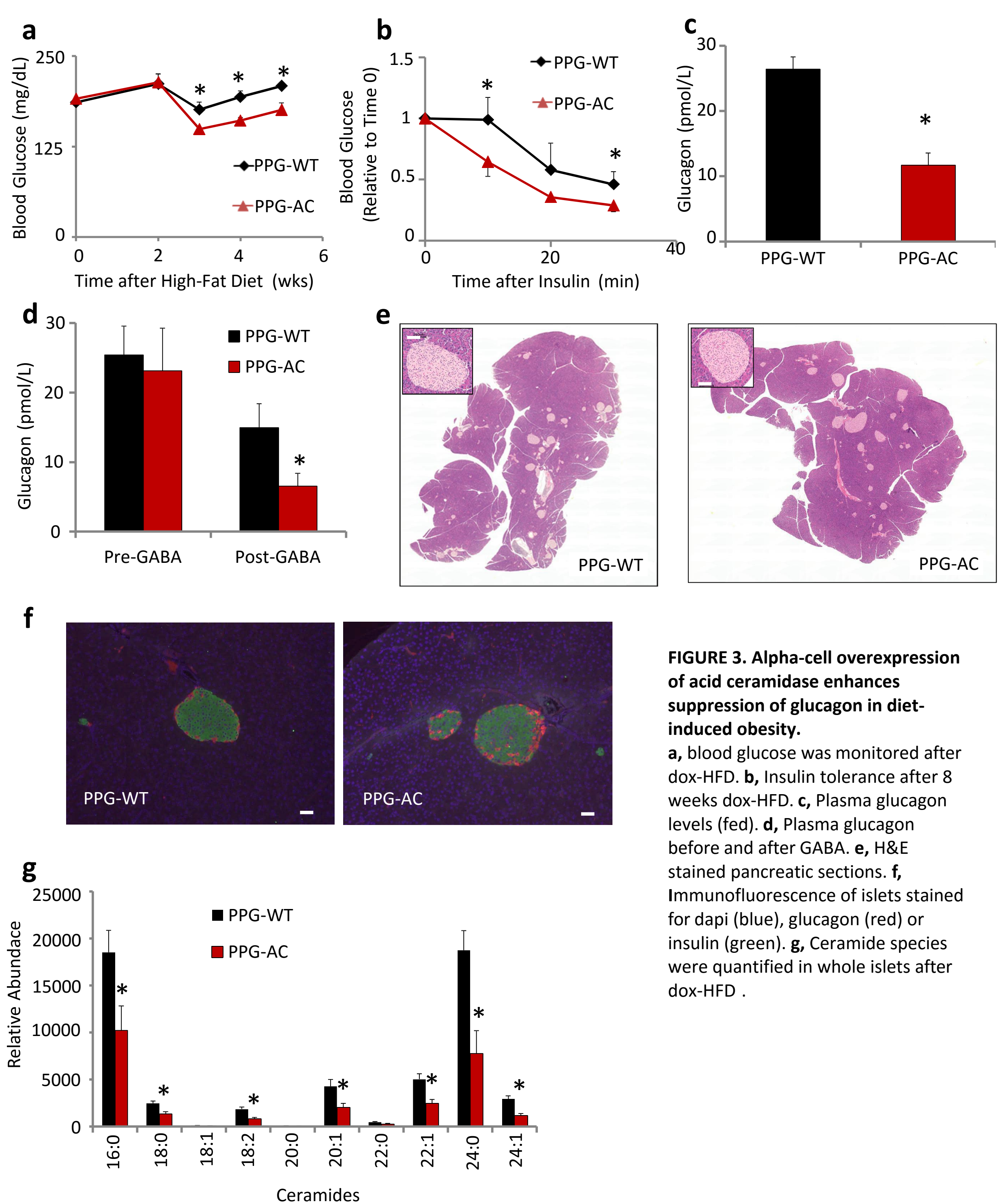
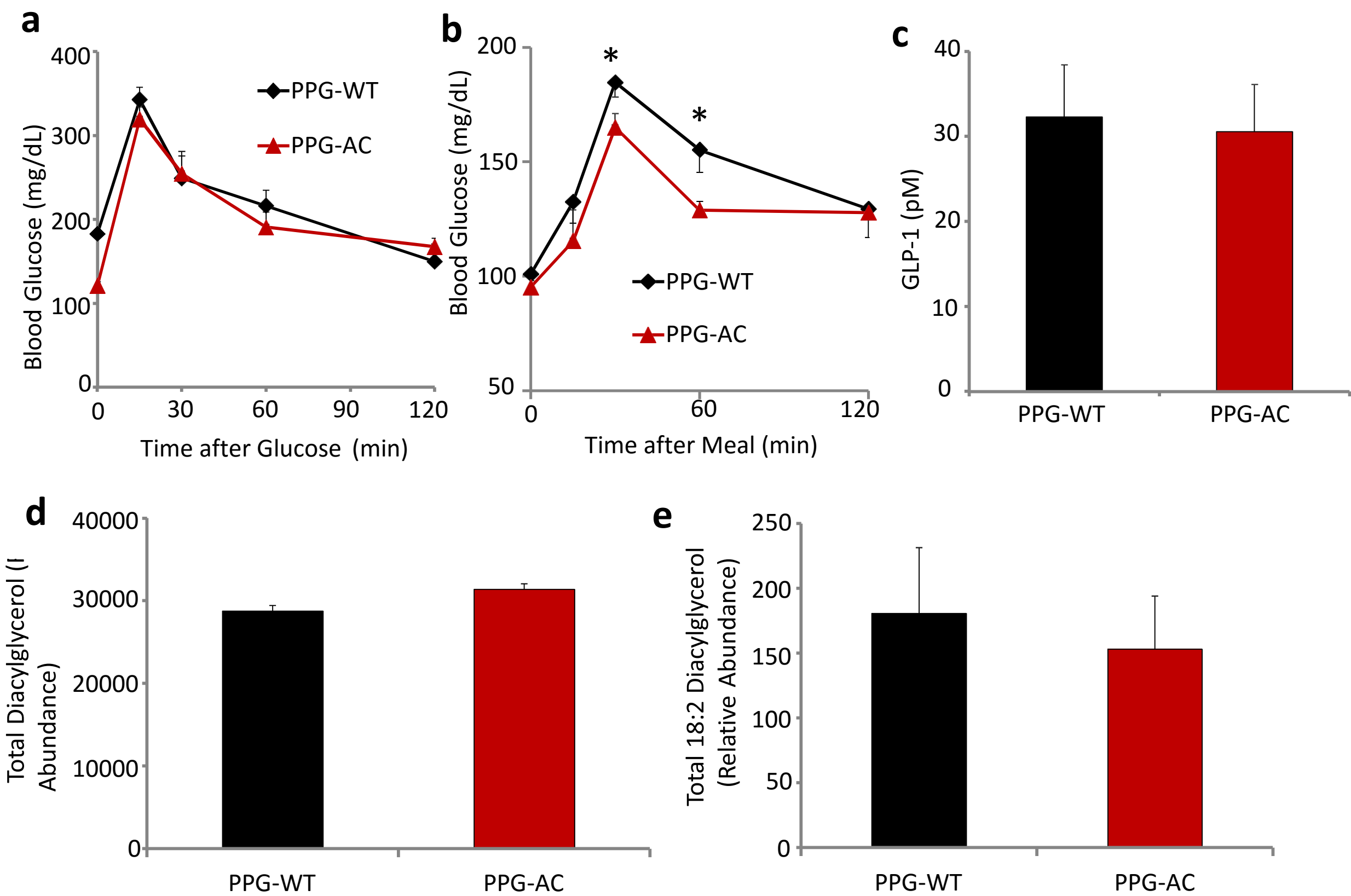


FIGURE 3. Alpha-cell overexpression of acid ceramidase enhances suppression of glucagon in diet-induced obesity.

a, blood glucose was monitored after dox-HFD. **b**, Insulin tolerance after 8 weeks dox-HFD. **c**, Plasma glucagon levels (fed). **d**, Plasma glucagon before and after GABA. **e**, H&E stained pancreatic sections. **f**, Immunofluorescence of islets stained for dapi (blue), glucagon (red) or insulin (green). **g**, Ceramide species were quantified in whole islets after dox-HFD.



EXTENDED DATA FIGURE 3. **a**, Blood glucose levels were measured during an oral glucose tolerance test. **b**, Blood glucose after oral gavage of mixed meal (Ensure). **c**, Plasma GLP-1 levels. **d**, Total DAG species and **e**, 18:2 DAG species were quantified in whole islets. n=6/group. *Denotes p<0.05

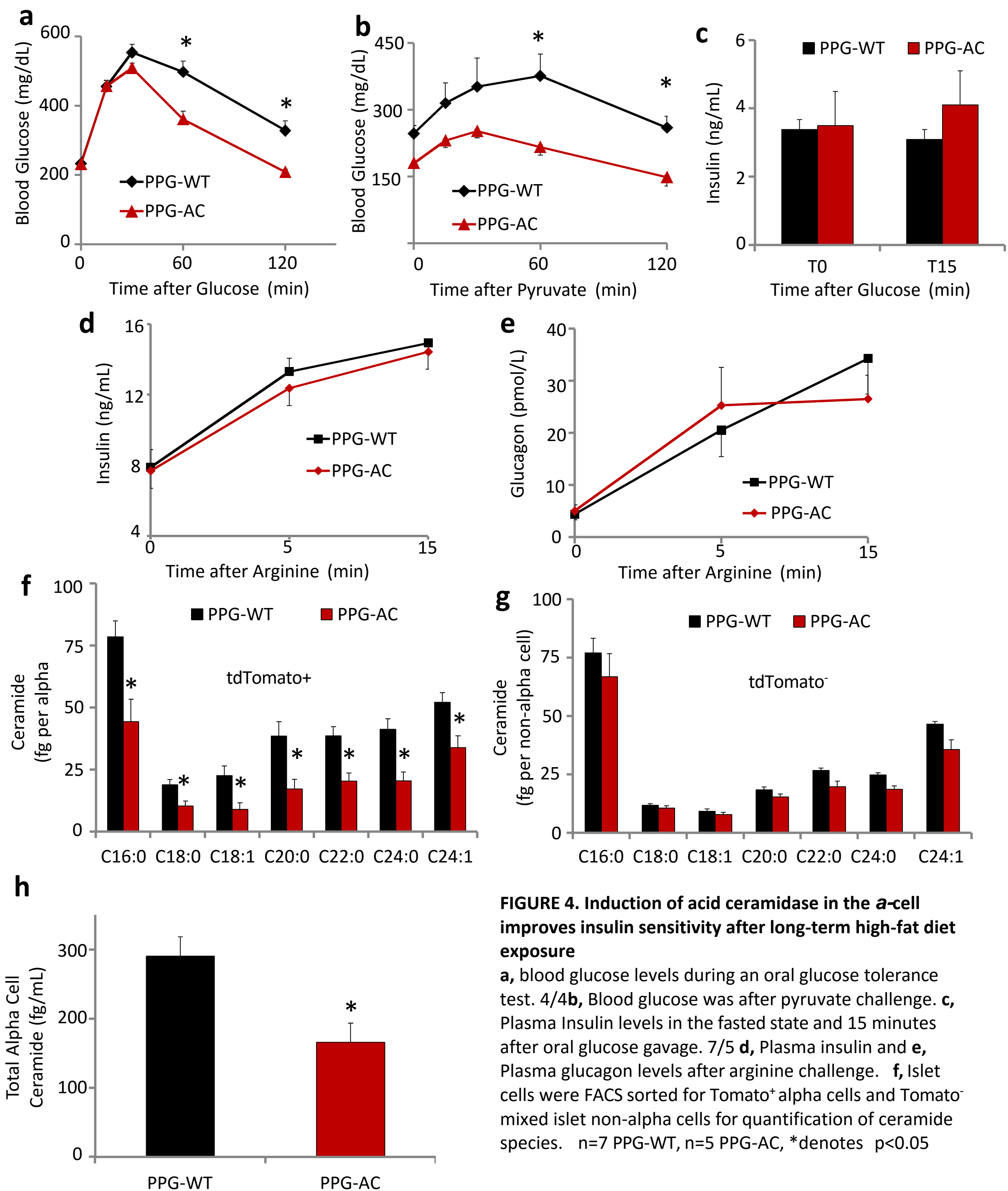
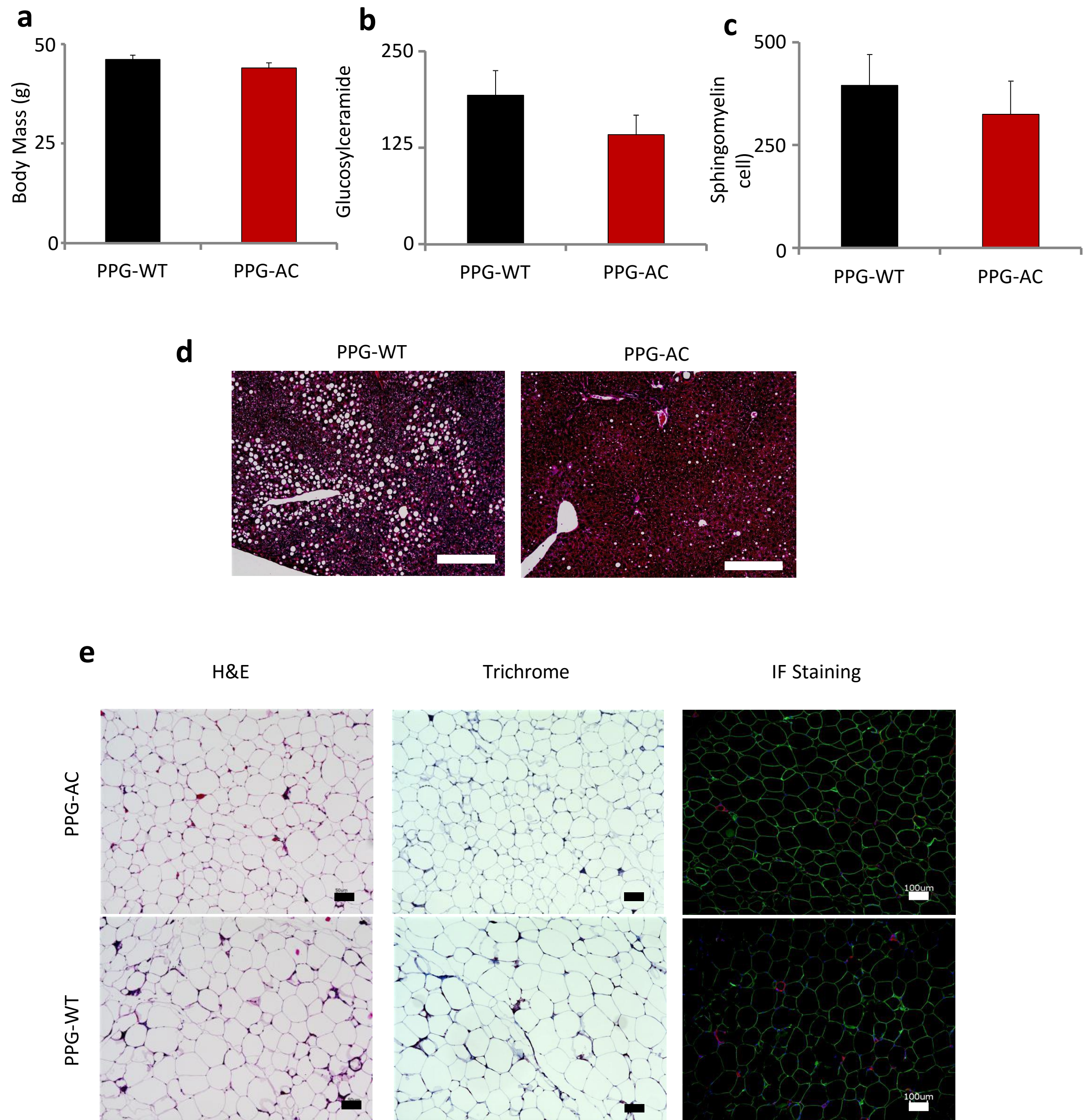


FIGURE 4. Induction of acid ceramidase in the α -cell improves insulin sensitivity after long-term high-fat diet exposure

a, blood glucose levels during an oral glucose tolerance test. **b**, Blood glucose was after pyruvate challenge. **c**, Plasma Insulin levels in the fasted state and 15 minutes after oral glucose gavage. **d**, Plasma insulin and **e**, Plasma glucagon levels after arginine challenge. **f**, Islet cells were FACS sorted for Tomato⁺ alpha cells and Tomato⁻ mixed islet non-alpha cells for quantification of ceramide species. n=7 PPG-WT, n=5 PPG-AC, *denotes p<0.05



EXTENDED DATA FIGURE 4. **a**, Body weights after 10-weeks of Dox-HFD. **b&c**, Quantification of total glucosylceramide (**b**) and sphingomyelin (**c**) species from tdTomato⁺ alpha cells . **d**, Representative H&E stained images of PPG-WT and PPG-AC livers (scale bars =300um). **e**, Representative H&E, Trichrome, and immunofluorescence of gonadal white adipose tissue (scale bars=100um).

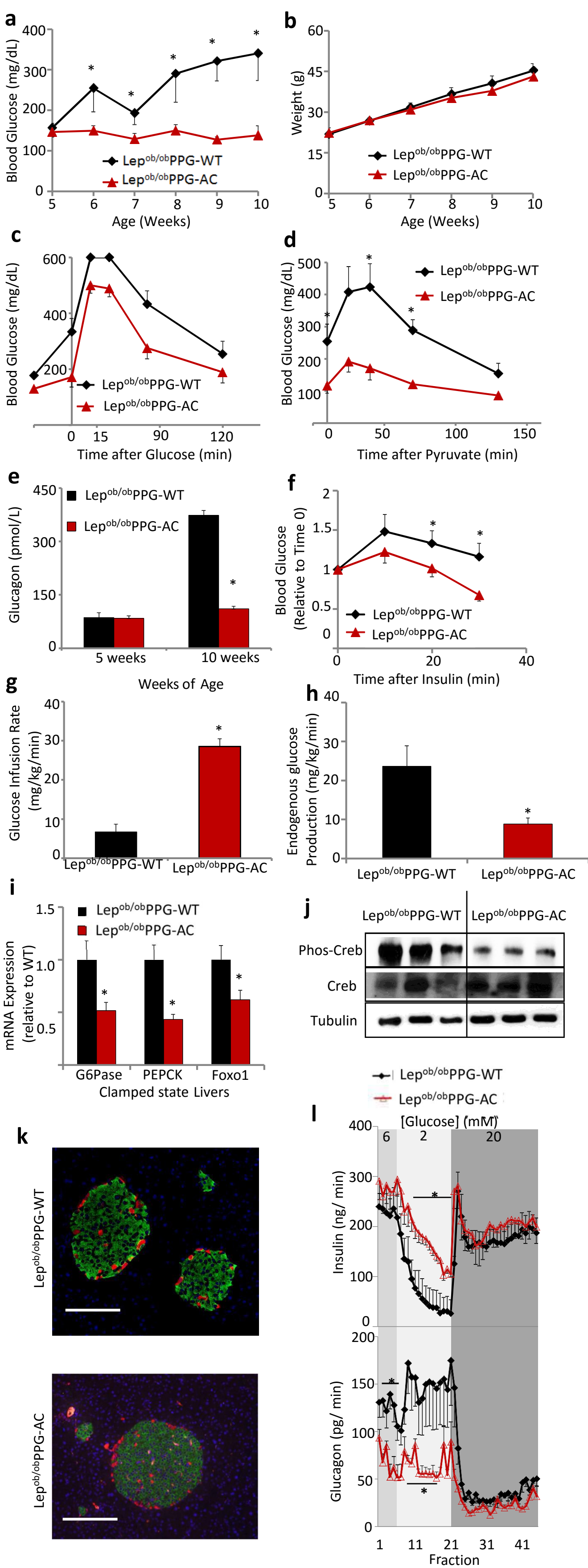


FIGURE 5. Overexpression of acid ceramidase in the α -cell of $Lep^{ob/ob}$ mice prevents hyperglycemia and hyperglucagonemia
a, Blood glucose and **(b)** body mass were monitored after dox -chow. **c**, Blood glucose levels during an oral glucose tolerance test. **d**, Blood glucose was monitored after pyruvate challenge. **e**, Plasma glucagon before dox and after 7 weeks of dox. **f**, Circulating glucose levels after insulin challenge. **g**, Glucose infusion rates and **(h)** hepatic glucose output during hyperinsulinemic-euglycemic clamps. **i**, Relative abundance of G6Pase, PEPCK, and Foxo1 mRNA from liver following clamp studies. **j**, Representative immunoblots of phosphorylated and total Creb of livers from clamped state mice, shown in triplicate. **k**, Insulin (green), dapi (blue) and glucagon (red) immunofluorescence of the islet. **l**, Insulin (top) and Glucagon (bottom) quantified from pancreatic perfusate under 6, 2, or 30 mM glucose (n=4). n=7 $Lep^{ob/ob}$ PPG-WT, n= 5 $Lep^{ob/ob}$ PPG-AC. *denotes p<0.05.

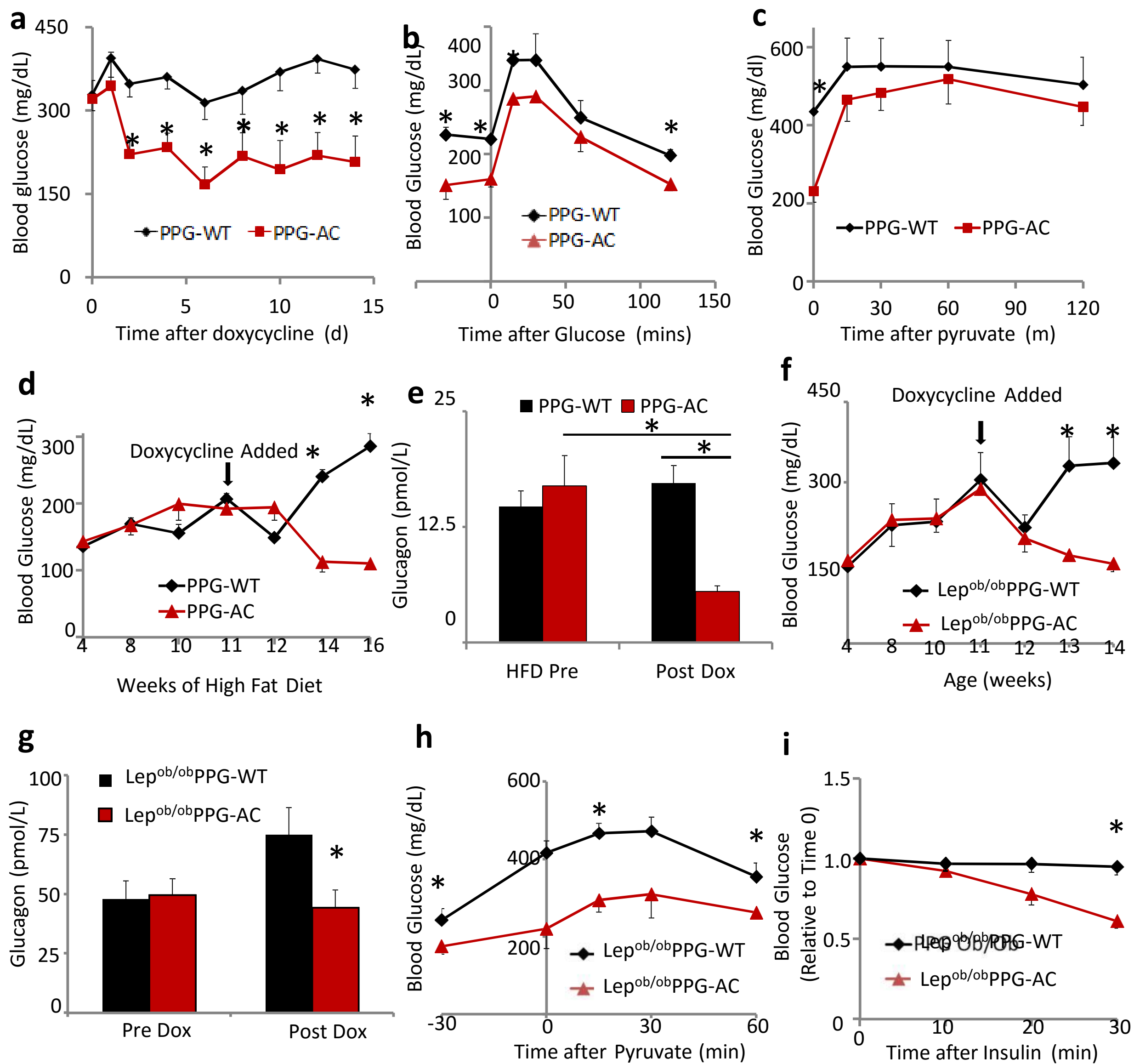


FIGURE 6. Inducing acid ceramidase overexpression in the α -cell of obese diabetic mice reverses hyperglycemia

a, Blood glucose was monitored after dox-HFD was provided to HFD-STZ diabetic mice (n= 4 PPG-WT, n=5 PPG-AC). **b**, Blood glucose after oral glucose challenge. **c**, Blood glucose after pyruvate challenge. **d**, Blood glucose during HFD was monitored. (n=5 PPG-AC, n=6 PPG-WT) **e**, Plasma glucagon pre and post dox-HFD. **f**, Blood glucose of Lep^{ob/ob}PPG-WT and Lep^{ob/ob}PPG-AC mice was monitored for 14 weeks (n=5 each group). **g**, Plasma glucagon was quantified pre and post dox-chow. **h**, Blood glucose after pyruvate challenge performed at 14 weeks of age. **i**, Blood glucose levels during insulin tolerance test. * denotes p<0.05

Chapter 3

Adiponectin Receptors and FGF21

Adiponectin and its receptors 1 and 2 (AdipoR1/R2) have been shown to promote ceramidase activity in many cell types (1). Their lipid targets for catabolism, ceramides and glucosylceramides, play causal roles in impairing insulin signaling. By promoting adiponectin secretion or overexpressing AdipoR1/R2 in an adipose or liver specific manner can improve hepatic steatosis and whole body glucose homeostasis (1,2). It has been demonstrated that Fibroblast growth factor 21 (FGF21) rapidly promotes the secretion of adiponectin, and subsequently increases the degradation of ceramide species. The alpha cell specific lowering of ceramides, via acid ceramidase overexpression, shows a regulation of glucagon secretion. The following preliminary data supports our previous model of glucagon regulation or could elucidate a parallel pathway, where FGF21 is acting independently of adiponectin to regulate glucagon secretion.

Introduction

Ceramides and glucosylceramides are part of an important class of bioactive sphingolipids, and have been implicated in regulating many cellular processes. Their over accumulation has led to the disruption of many cellular processes and have been implicated in many metabolic disorders, including atherosclerosis, insulin resistance, lipotoxic heart failure, beta-cell apoptosis, and beta-cell dysfunction (3). Also, sphingolipid metabolites have been shown to accumulate in the islets of diabetic rodents (4). Our recent unpublished data shows that the aberrant accrual of ceramides within the alpha cell can propagate hyperglucagonemia

and subsequently hyperglycemia in diet induced obese mouse models and subsequent ablation of these lipotoxic molecules can reverse and prevent this phenotype. It has been shown that the adipokine, adiponectin, and fibroblast growth factor 21 (FGF21) serve, in part, to lower sphingolipids in tissues (5). Yet, it is still unclear the roles adiponectin and FGF21 may play as regulators of glucagon secretion.

The adipocyte secreted protein, adiponectin, has been shown to ameliorate hyperglycemia, insulin resistance, and hyperlipidemia in diabetic mice (6,7,8). Many of these effects can be attributed to the concomitant ceramide-lowering potential of the adiponectin receptors 1 and 2 (AdipoR1/R2). These two receptor isoforms have been shown to induce ceramidase activity. Ceramidase hydrolyzes ceramide into sphingosine and free fatty acid. Subsequent phosphorylation of sphingosine by its kinase produces sphingosine-1-phosphate (S1P)—a signaling molecule that contributes to the processes of cell signaling, proliferation, survival, and metabolism (9). More notably, S1P can make substantial increases in glucose-stimulated insulin secretion (GSIS) in pancreatic beta cells (10). However, these effects cannot directly link the canonical associated adiponectin increases in activity of AMP-activated protein kinase (AMPK) to these ceramide lowering effects (11). To further our understanding of adiponectin signaling in the alpha cell, we have generated alpha cell specific mouse models allowing for AdipoR2 to be expressed under the control of a tetracycline response element (TRE-AdipoR2)(Extended Figure 1a). The PPG-rtTA will drive alpha- cell specificity to limit ceramide accumulation within the alpha cell, possibly increasing S1P, and blunting glucagon secretion.

As a potent adiponectin secretagogue, fibroblast growth factor 21 (FGF21) has also demonstrated ceramide lowering effects. FGF21 signals through its co-receptors, FGF receptors (FGFRs) and beta-klotho (KLB). The FGFRs cover a wide variety of tissues, but many are not tissue specific. However, tissue specific knockouts of the coreceptor beta-klotho can reveal FGF21's function in a target tissue. Several studies have shown that an upregulation of FGF21 expression exhibits many beneficial metabolic effects, including the suppression of glucagon (12,13,14). To assess FGF21 signaling in the alpha cell, we have generated an alpha cell specific mouse model to flox-out the coreceptor, KLB, which will be inducibly deleted by tetracycline response element driven expression of Cre Recombinase (TRE-Cre) (Extended Figure 1B). These preliminary data generated from these independent mouse models will discern the mechanisms by which adiponectin and FGF21 suppress glucagon.

Results

Adiponectin ameliorates hyperglycemia and hyperglucagonemia via induction of ceramidase activity

The small-molecule, AdipoRon, is an adiponectin receptor (AdipoR) agonist and has been demonstrated to improve insulin resistance, dyslipidemia, and glucose intolerance in db/db mice (15). Promoting ceramide accumulation within cultured InR1G9 alpha cells via incubation of the saturated fatty acid palmitate, drove glucagon secretion in the absence of AdipoRon even when insulin is present. However, with the addition of this AdipoR agonist, glucagon secretion is reduced by 36% compared to palmitate and insulin treatment alone (Figure 1a). Since AdipoRon has the propensity to behave like recombinant adiponectin, we will

continue to perform assays to measure ceramidase activity, signaling pathways intermediates, and its ability to lower ceramides *in vitro*.

In Vivo, a single intraperitoneal dose of AdipoRon lowers ceramides in the hypothalamus and liver of Lep^{ob/ob} mice (Figure 1b). However, AdipoRon's effects in either isolated islets or cultured alpha cells have not been reported. To test whether increased AdipoR activity has a functional role in ceramide metabolism and subsequent glucagon secretion in the alpha cell, we crossed the preproglucagon tetracycline-controlled transactivator (PPG-rtTA) and Tet-responsive (TRE-R2) onto the Lep^{ob/ob} background. At 5-weeks of age, Lep^{ob/ob}-WT and Lep^{ob/ob}-R2 mice were placed on a doxycycline diet. Blood glucoses at the beginning of the diet were equivalent, but only the Lep^{ob/ob}-R2 remained refractory to hyperglycemia over the 10-week period (Figure 1c). Serum glucagon levels at 5- and 10-weeks of age were reported (Figure 1d), and circulating glucagon levels are significantly decreased in the Lep^{ob/ob}-R2 mice at 10-weeks. Levels of circulating insulin are unchanged compared to WT mice (Extended Figure 1b). During glucose challenge (Figure 1e), Lep^{ob/ob}-R2 mice have a greater clearance of circulating glucose compared to their WT counterparts. Trending improvements in gluconeogenesis, measured by pyruvate challenge, were seen (Figure 1f).

During insulin tolerance test, Lep^{ob/ob}-R2 mice have a significant improvement to lower blood glucose (Figure 1g). To assess whole-body insulin sensitivity, we performed hyperinsulinemic-euglycemic clamps. The glucose infusion rate was 3.7-fold greater in Lep^{ob/ob}-R2 mice (Figure 1h). This increase of glucose infusion to maintain euglycemia at approximately 150mg/dL in the clamped state could be due to the lower abundance of circulating glucagon in the pre- and post-clamp state (Extended Figure 1c). Hepatic glucose output in these mice still

needs to be measured. Arginine induced secretion of insulin and glucagon (Figure 1i&j) is altered in Lep^{ob/ob}-R2 mice.

Pancreatic sections were taken and stained by immunofluorescence (Figure 1j). These representative pictures indicate an increase in islet size, but further investigation of H&E stained sections to measure islet mass is needed. AdipoR2 overexpression has been shown to increase sphingosine-1-phosphate (S1P) levels in hepatocytes (2). This increase in S1P can promote the survival and proliferation of the islet and also activate AMPK, and both might contribute to the increase in islet mass. Cultured alpha cells, isolated islets, and isolated alpha cells will be used to further elucidate these hypotheses.

FGF21 independently degrades ceramides and blunts glucagon secretion *In Vitro*

To investigate the role of FGF21 in cultured alpha cells, the saturated fatty acid palmitate was used to provide substrate for de novo ceramide synthesis (Figure 2a). FGF21 alone, in the absence of adiponectin, has the ability to lower ceramides even when challenged with palmitate. Glucagon secretion (Figure 2b) was also measured, and is blunted with the addition of FGF21. The ability to break down ceramides without the signaling efforts of adiponectin can possibly be explained by an increase of lipid oxidation. However, these data may suggest a parallel pathway by which FGF21 is signaling within the alpha cell.

Endogenous beta-klotho (KLB) expression using a TdTomato reporter, mediated by a CRISPR knock-in model, is located on the periphery of the islet where alpha cells in the mouse islet are located (Figure 2c). Furthermore, pErk1/2 immunofluorescence (IF) was measured after vehicle or FGF21 infusion (Figure 2d). Again, high levels of pErk1/2 expression is localized

on the cortex of the islet. These data suggest that the alpha cell is a major target for FGF21 signaling.

Alpha cell specific deletion of the FGF21 coreceptor, beta-klotho, exhibits increases in circulating factors

PPG-rtTa was crossed with a Tet-activated cre-recombinase (TRE-Cre), a loxp-flanked KLB allele, and the PANIC-attac mouse model to inducibly knockout KLB from alpha cells of mice. The PANIC-attac model is used to titratably induce beta-cell apoptosis with the administration of dimerizer (AP20187) (need ref). Mice were given doxycycline diet to knockout KLB prior to beta-cell ablation. Glucose levels 10-days post dimerizer administration were equivalent between each group (Figure 3a). However, circulating levels of glucagon (Figure 3b), C-peptide (Figure 3c), and insulin (Figure 3d) were higher in the PPG KLB KO group.

Diet Induced Obesity decreases insulin sensitivity in beta-klotho deficient knockout mice

To assess FGF21's effects in a diet induced obesity model, PPG KLB KO mice were placed on a high-fat doxycycline diet for 8-weeks. Fed circulating insulin (Figure 4a) and glucagon (Figure 4b) levels were significantly increased in PPG KLB KO mice. Compared to WT mice, PPG KLB KO mice also have impairments in insulin sensitivity (Figure 4c) and glucose tolerance (Figure 4d). A trend in diminished glucose excursion is measure by pyruvate challenge (Figure 4e). The enhanced secretion of glucagon and insulin induced by arginine (Figure 4f&g) illustrates an altered secretory capacity.

Methods and Animals

All animal experimental protocols were approved by the Institutional Animal Care and Use Committee of University of Texas Southwestern Medical Center at Dallas. All overexpression experiments were performed in a pure C57/Bl6 background. All experiments were conducted using littermate-controlled male mice, with the exception of Lep^{ob/ob} studies which used equivalent numbers of male and female Lep^{ob/ob} mice in each cohort. Preproglucagon (PPG)-rtTA mice were previously generated containing the 1.7-kb PPG promoter [CK]. This mouse was subsequently crossed to the TRE-R2 transgenic mice previously described [JX]. All Dox-chow diet (600 mg/kg Dox) or HFD-Dox (600 mg/kg Dox) experiments were performed with identical diets given to control and transgenic littermates. High fat diets (60% fat by caloric content) were compounded with doxycycline and sterilized (Bioserv). To achieve diabetes in high-fat fed mice, animals were fasted for 6 hrs and subjected to injection of STZ (65 mg/kg, IP) once weekly for 5 weeks during weeks 3-8 after starting high fat diet ([Ye et al., 2014](#)).

Systemic tests

For oral glucose tolerance tests, mice were fasted for 4 hours prior to administration of glucose (2.5 g/kg body-weight by gastric gavage). Glucose levels were measured by glucometer (Bayer Contour) and plasma was collected before glucose and 15 minutes after glucose administration. Mice did not have access to food throughout the experiment. Pyruvate was administered 1g/kg body weight by intraperitoneal injection following overnight removal of high fat diet or 4-hour removal of chow diet from Lep^{ob/ob}. For the arginine tolerance test, HFD mice were fasted overnight (12–16 h) and Lep^{ob/ob} mice were fasted for 4 hours before intraperitoneal injection of L-arginine 1 g/kg body weight. Insulin tolerance tests were initiated by intraperitoneal injection of 0.75 U/kg (lean and HFDrecombinant human insulin (humalin-R, Lilly)

Plasma Parameters

For glucagon measurement plasma was collected with aprotinin, and glucagon levels were measured by using an ELISA kit (Merckodia Inc., Winston-Salem, NC). Insulin levels were measured using commercial ELISA kits (Crystal Chem).

Hyperinsulinemic-clamps

Hyperinsulinemic-euglycemic clamps were performed on conscious, unrestrained Lepo^{ob/ob} mice as previously described (19, 37). Hyperinsulinemic-hypoglycemic clamps were performed as previously described⁸. For both studies hyperinsulinemia was initiated by primed-continuous infusion of insulin (10 mU/kg/min).

Glucagon Secretion assays

InR1G9 cells were treated with and without 500uM palmitate for 18 hours with and without 5mg/kg AdipoRon or recominant FGF21 at 1ug/mL. Ceramides were measured by shotgun lipidomics (n=4 each group). InR1G9 treated cells with and without C2 ceramide and palmitate. Glucagon secretion is reported as a percent of control. (n= 4 each group) InR1G9 cells were treated with and without C2 ceramide and with and without 250nM insulin.

Histology and immunofluorescence (IF)

Tissues were excised and fixed in 10% PBS buffered formalin for 24 h. Following paraffin embedding and sectioning (5 µm), tissues were stained with H&E or a Masson's trichrome stain. For IF, paraffin-embedded sections were stained using monoclonal antibodies to Insulin (1:500, A0564, DAKO Products) and Glucagon (1:250, ab10988, Abcam).

Lipid Quantification

Sample Preparation. Flash frozen cell pellets (2x10⁶ cells per sample) in a borosilicate glass tube were quenched with 2.0 mL of organic extraction solvent (isopropanol: ethyl acetate, 15:85; vol:vol). Immediately afterwards, 20 µL of internal standard solution was added (Avanti Polar Lipids, AL Ceramide/Sphingoid Internal Standard Mixture II diluted 1:10 in ethanol). The mixture was vortexed and sonicated in ultrasonic bath during 10 minutes at 40 °C. Then the samples were allowed to reach room temperature and 2 mL of HPLC water was added. Two-phase liquid extraction was performed, the upper phase was transferred to a new tube and the pellet was re-extracted. Supernatants were combined and evaporated under nitrogen. The dried residue was reconstituted in 2.0 mL of Folch solution, 400 µL were transferred to a new tube and were reserved for organic phosphate determination, 300 µL were transferred to a new tube and were reserved for infusion based LC-MS analysis, the remaining volume was reserved for targeted LC/MS/MS sphingolipid analysis. The different organic fractions were dried under nitrogen and stored at -80C until analysis.

Sphingolipid Analysis. Sphingolipids levels were quantitated using LC/MS/MS methodology using a Nexera X2 UHPLC system coupled to a Shimadzu LCMS-8050 triple quadrupole mass spectrometer operating the Dual Ion Source in Electrospray positive mode.^{1,2} Dried lipid extracts were reconstituted in 200 µL of HPLC solvent (methanol/ formic acid 99:1; vol:vol containing 5 mM ammonium formate) for LC-MS/MS analysis. Lipid separation was achieved on a 2.1 (i.d.) x 150 mm Kinetex C8, 2.6 micron core-shell particle (Phenomenex, Torrance, CA) column.

Sphingolipids species were identified based on exact mass and fragmentation patterns, and verified by lipid standards. The concentration of each metabolite was determined according to calibration curves using peak-area ratio of analyte vs. corresponding internal standard.

Calibration curves were generated using serial dilutions of each target analyte. Sphingolipid true standards were purchased from Avanti Polar Lipids (Alabaster, Al).

Total Phosphorous Determination. Total phosphorous content in the organic extracts was determined as described by Chen et al., and Fiske and Subbarow.^{3,4}

Statistics

The results are shown as mean±SEM. All statistical analysis was performed in SigmaStat 2.03 (SysStat Software, Point Richmond, CA). Differences between the two groups over time (indicated in the relevant figure legends) were determined by a two-way analysis of variance for repeated measures. For comparisons between two independent groups, a Student's t test was used. Significance was accepted at $P < 0.05$.

1. Holland WL, Miller RA, Wang ZV, Sun K, Barth BM, Bui HH, et al. Receptor-mediated activation of ceramidase activity initiates the pleiotropic actions of adiponectin. *Nature medicine*. 2011;17(1):55-63. Epub 2010/12/28. doi: nm.2277 [pii]10.1038/nm.2277. PubMed PMID: 21186369.
2. Xia JY, Holland WL, Kusminski CM, Sun K, Sharma AX, Pearson MJ, et al. Targeted Induction of Ceramide Degradation Reveals Roles for Ceramides in Non Alcoholic Fatty Liver Disease and Glucose Metabolism in Mice. *Cell Metab*. 2015;22(2):266-76. doi: 10.1016/j.cmet.2015.06.007. PMID: 26190650.
3. Holland WL, Summers SA. Sphingolipids, insulin resistance, and metabolic disease: new insights from in vivo manipulation of sphingolipid metabolism. *Endocr Rev*. 2008;29(4):381-402. PubMed PMID: 18451260.
4. Shimabukuro M, Higa M, Zhou YT, Wang MY, Newgard CB, Unger RH. Lipoapoptosis in beta-cells of obese prediabetic fa/fa rats. Role of serine palmitoyltransferase overexpression. *The Journal of biological chemistry*. 1998;273(49):32487-90. Epub 1998/11/26. PubMed PMID: 9829981.
5. Lin Z, Tian H, Lam KS, Lin S, Hoo RC, Konishi M, et al. Adiponectin Mediates the Metabolic Effects of FGF21 on Glucose Homeostasis and Insulin Sensitivity in Mice. *Cell Metab*. 2013;17(5):779-89. doi: 10.1016/j.cmet.2013.04.005. PubMed PMID: 23663741.
6. Shklyayev, S. *et al*. Sustained peripheral expression of transgene adiponectin offsets the development of diet-induced obesity in rats. *Proc. Natl Acad. Sci*. 2003 USA 100, 14217–14222.
7. Berg, A. H. , Combs, T. P. , Du, X. , Brownlee, M. & Scherer, P. E. The adipocyte-secreted protein Acrp30 enhances hepatic insulin action. *Nat. Med*. 2001;7, 947–953.
8. Yamauchi, T. *et al*. The fat-derived hormone adiponectin reverses insulin resistance associated with both lipoatrophy and obesity. *Nat. Med*. 2001;7, 941–946.
9. Hla T, Dannenberg AJ. Sphingolipid signaling in metabolic disorders. *Cell Metab* 2012;16: 420–434.
10. Stanford, JC. *et al*. Sphingosine 1-Phosphate (S1P) Regulates Glucose-stimulated Insulin Secretion in Pancreatic Beta Cells. *J. Biological Chemistry*. 2012; doi:10.1074/jbc.M111.268185.
11. Holland, William L. *et al*. The Pleiotropic Actions of Adiponectin Are Initiated via Receptor-Mediated Activation of Ceramidase Activity. *Nat. Med*. 17.1 (2011): 55–63.
12. Berglund ED, Li CY, Bina HA, Lynes SE, Michael MD, Shanafelt AB, et al. Fibroblast growth factor 21 controls glycemia via regulation of hepatic glucose flux and insulin sensitivity. *Endocrinology*. 2009;150(9):4084-93. Epub 2009/05/28. doi: en.2009-0221 [pii]10.1210/en.2009-0221. PubMed PMID:19470704.
13. Kharitonov A, Wroblewski VJ, Koester A, Chen YF, Clutinger CK, Tigno XT, et al. The metabolic state of diabetic monkeys is regulated by fibroblast growth factor-21. *Endocrinology*. 2007;148(2):774-81. Epub 2006/10/28. doi: 10.1210/en.2006-1168. PubMed PMID: 17068132.
14. Berglund ED, Unger RH. Role of fibroblast growth factor 21 in biology of glucagon. *Diabetes*. 2013;62(5):1376. doi: 10.2337/db12-1840. PubMed PMID: 23613555; PubMed Central PMCID: PMC3636638.
15. Okada-Iwabu M, Yamauchi T, Iwabu M, et al. A small-molecule AdipoR agonist for type 2 diabetes and short life in obesity. *Nature*. 2013;503 (7477): 493–9.

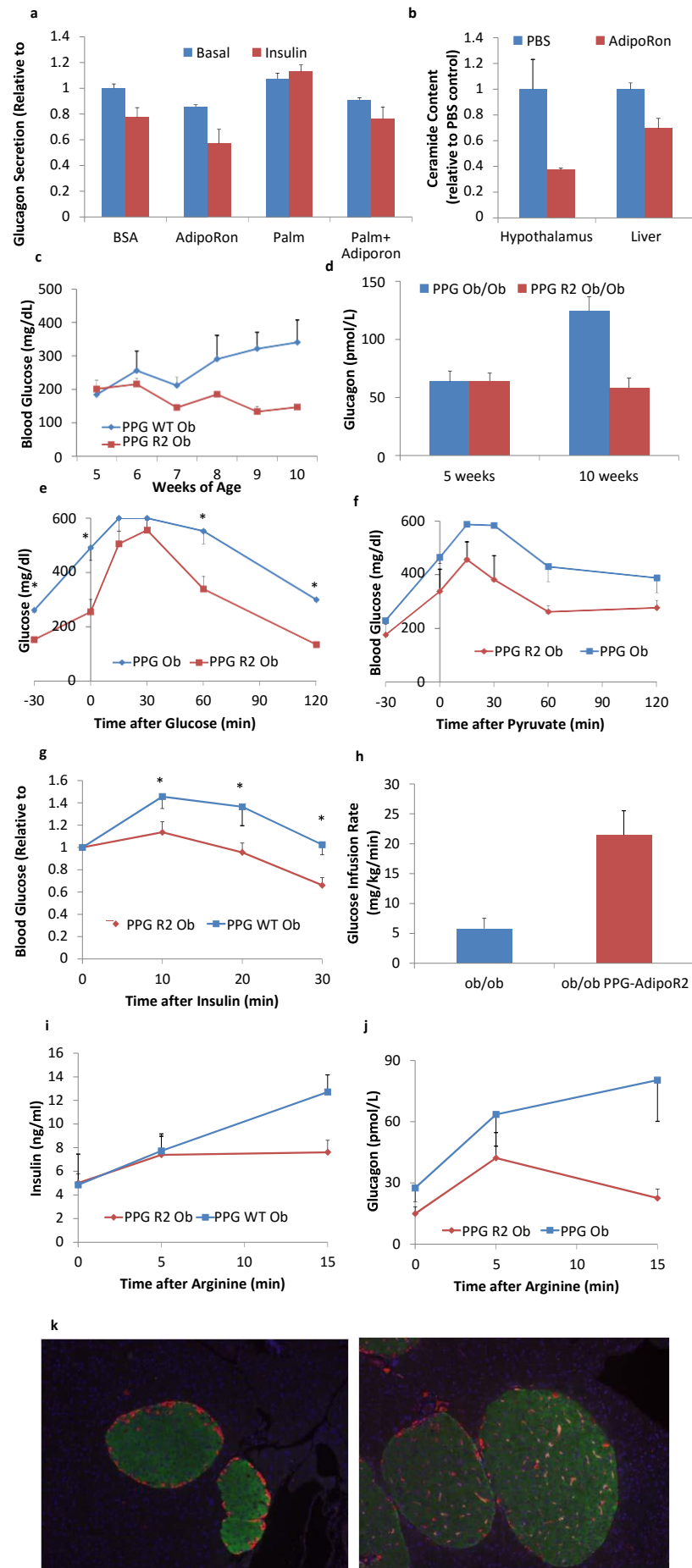


Figure 1. Adiponectin ameliorates hyperglycemia and hyperglucagonemia via induction of ceramidase activity
a, Glucagon secretion in to media was quantified and normalized to BSA control (n=4/group). **b**, Liver and hypothalamus ceramide content of mice treated with and without adipoRon (n=4/group). **c**, blood glucose was monitored during dox diet. **d**, Plasma glucagon before and after dox diet. **e**, Blood glucose levels were measured during an oral glucose tolerance test. **f**, Blood glucose was after pyruvate challenge. **g**, Insulin tolerance at 10-weeks. (n=5/4). **h**, Glucose infusion rates during clamps. (n=4/3). **i**, Plasma insulin and **j**, Plasma glucagon levels after arginine challenge. **k**, Immunofluorescence of islets stained for dapi (blue), glucagon (red) or insulin (green).

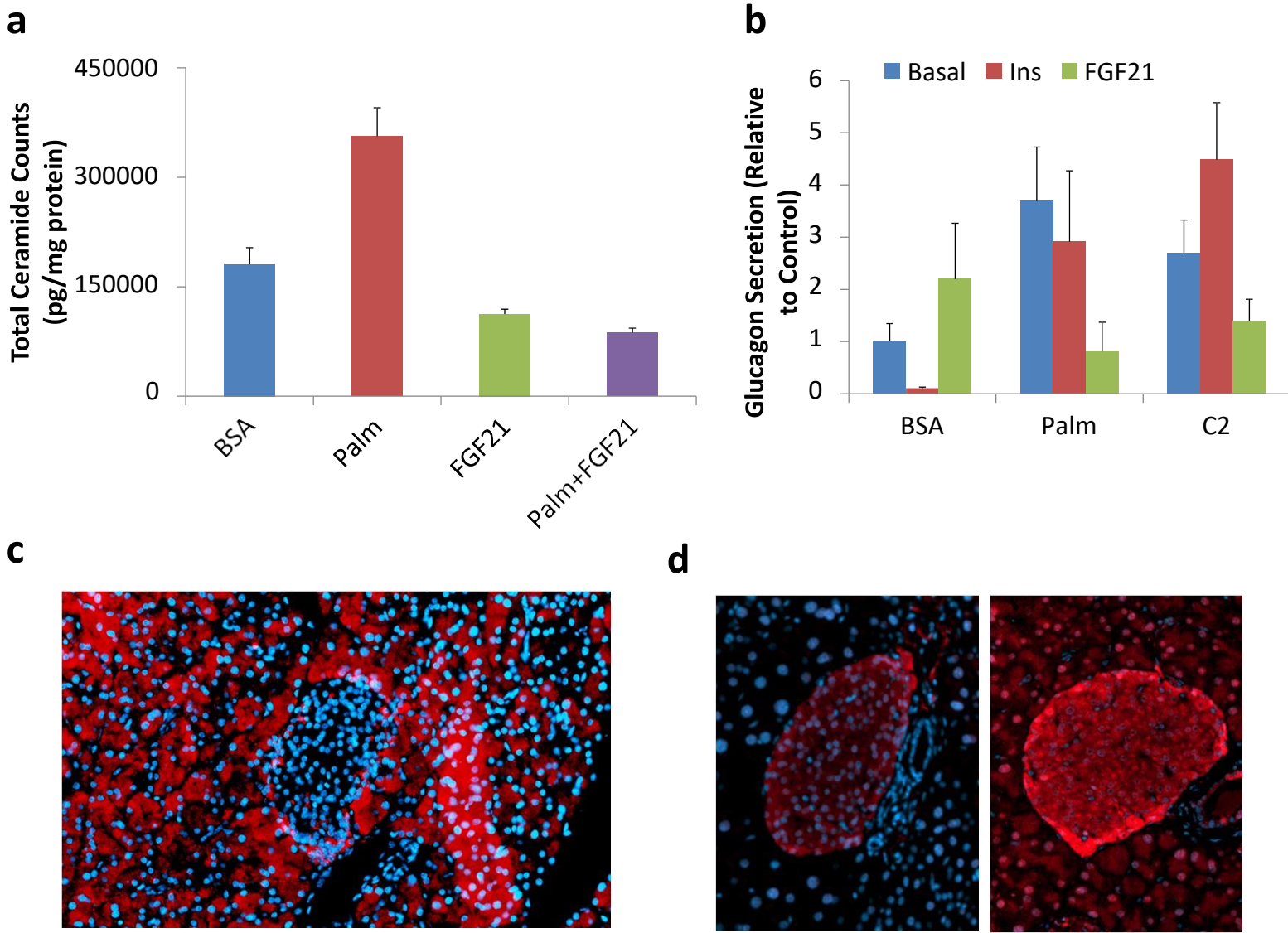


Figure 3. **FGF21 independently degrades ceramides and blunts glucagon secretion *In Vitro***
a-b, InR1G9 cells were treated with palmitate or fatty acid-free BSA in the presence or absence of FGF21.
a, Ceramide levels were quantitatively measured. **b**, Glucagon secretion into media was quantified and normalized to BSA control (n=4/group). **c**, FGF21 expression in pancreata via tdTomato reporter. **d**, immunofluorescence of islets for pERK1/2 (red) or DAPI (blue).

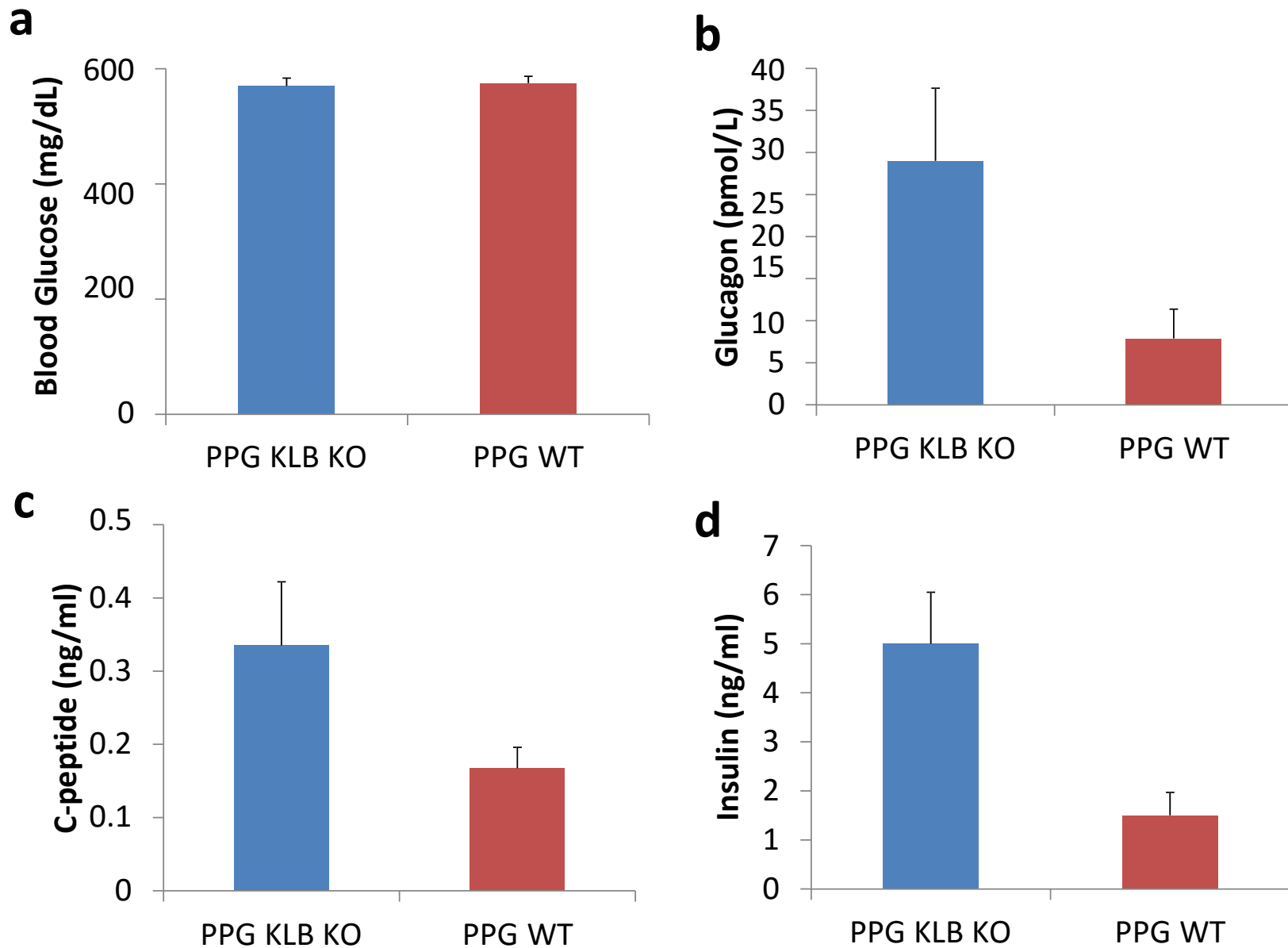


Figure 3. Alpha cell specific deletion of the FGF21 coreceptor, beta-klotho, exhibits increases in circulating factors

a, Blood glucose levels at time of sacrifice. **b-d**, 10-days post dimerization treatment and measure by ELISA. **b**, Plasma glucagon levels. **c**, Circulating C-peptide levels. **d**, Plasma insulin levels.

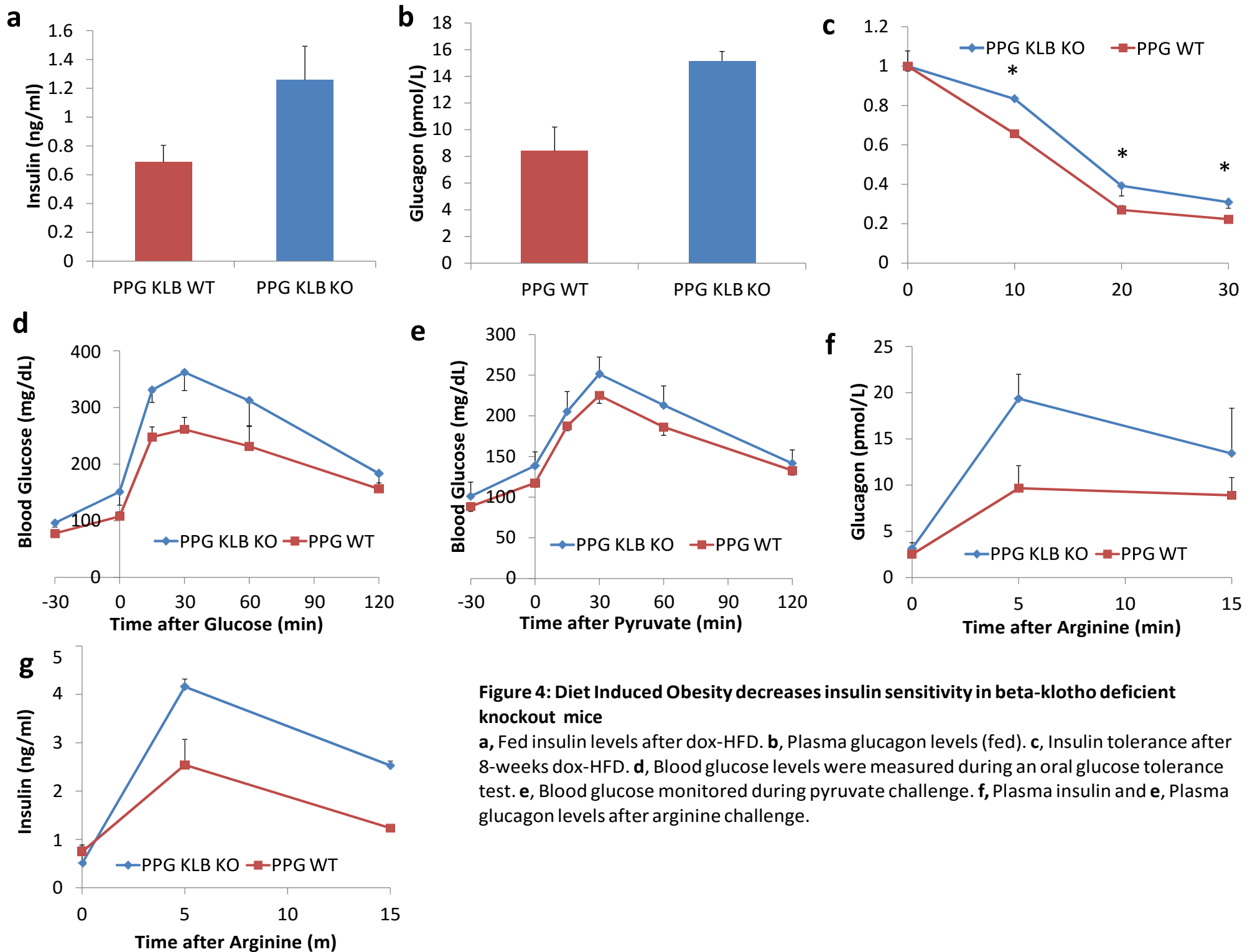
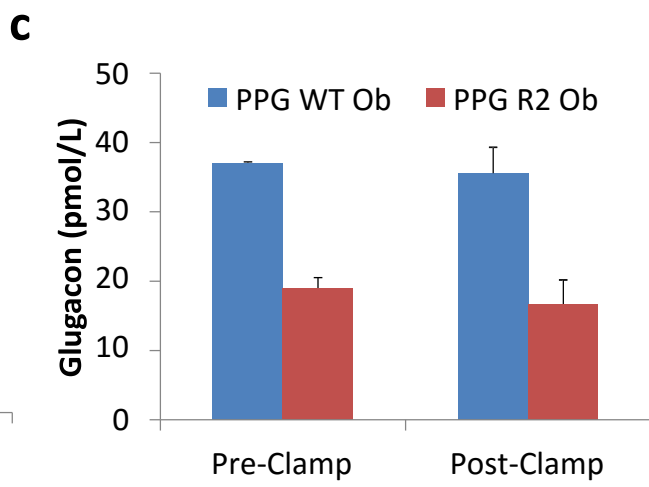
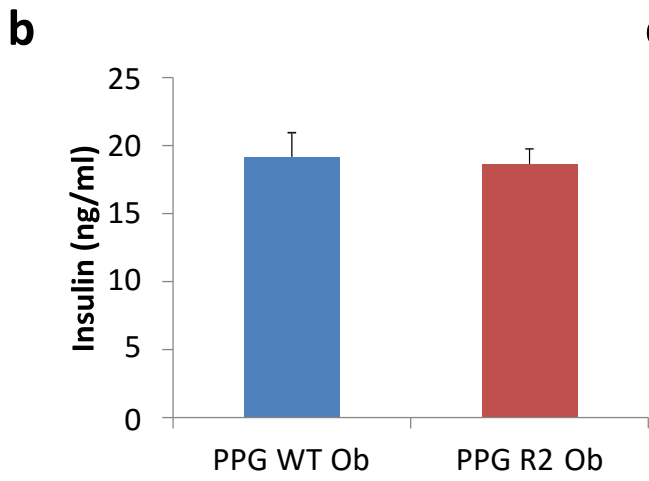
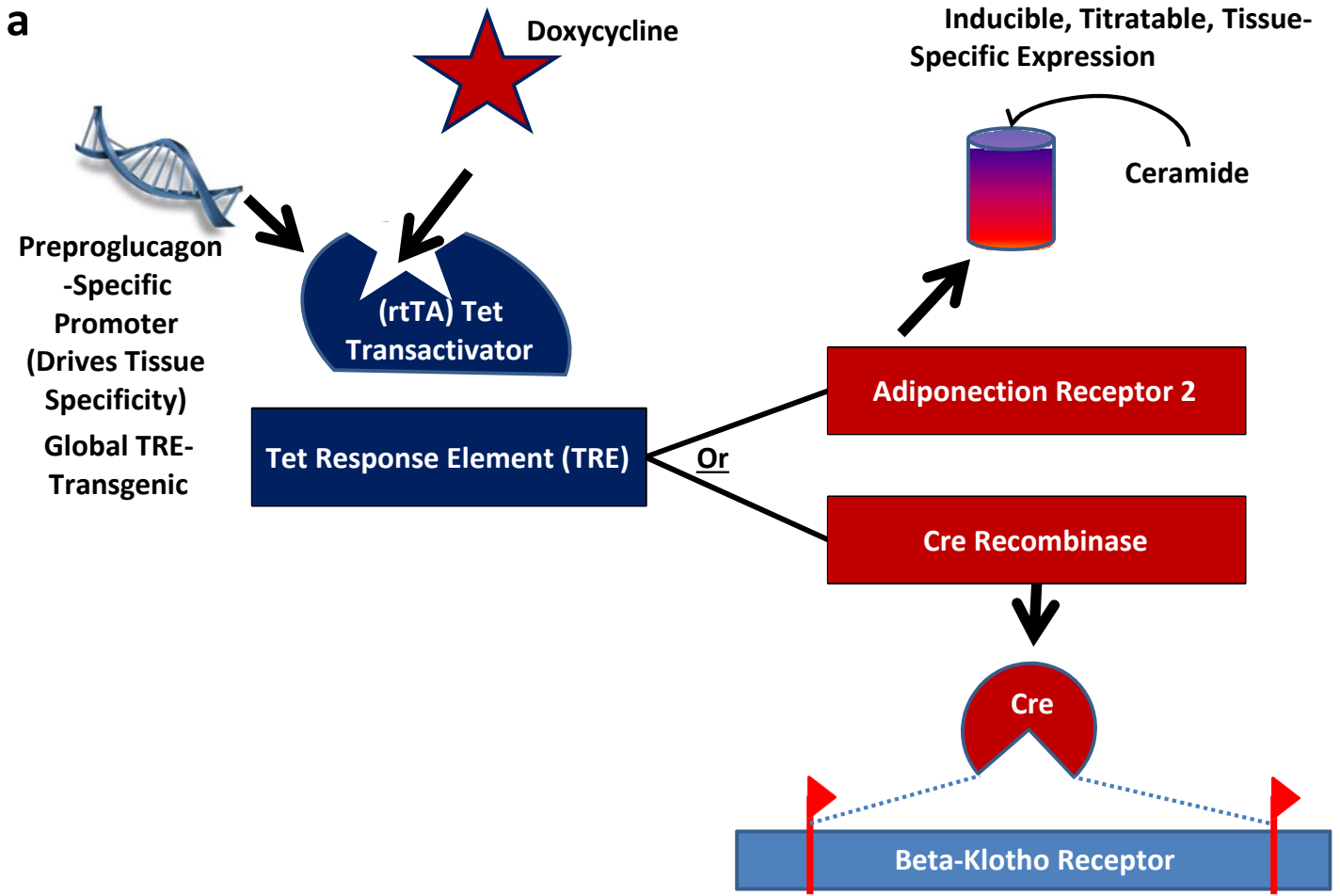


Figure 4: Diet Induced Obesity decreases insulin sensitivity in beta-klotho deficient knockout mice
a, Fed insulin levels after dox-HFD. **b**, Plasma glucagon levels (fed). **c**, Insulin tolerance after 8-weeks dox-HFD. **d**, Blood glucose levels were measured during an oral glucose tolerance test. **e**, Blood glucose monitored during pyruvate challenge. **f**, Plasma insulin and **e**, Plasma glucagon levels after arginine challenge.



Extended Figure 1. Mouse Model Representations and Insulin sensitivity in alpha cells

a. The schematic drawing depicts the alpha cell specific transgenic overexpression of adiponectin receptor 2 or deletion of the beta-klotho receptor induced and titrated by doxycycline diet. b. Circulating serum insulin levels at 10-weeks of age, measured by ELISA. c. Glucagon levels during the fasted (pre-clamp) and clamped state.

Chapter 4 Conclusions and Future Directions

Overexpression of the adiponectin receptor 2 has been shown to suppress glucagon in leptin deficient mice. In the acid ceramidase overexpression model, the argument is made that a reduction in Ca²⁺ signaling to decrease glucagon exocytosis via breakdown of ceramides in the alpha cell. However, one major difference between these two phenotypes are the arginine stimulated insulin and glucagon secretions. Are these ceramidases similarly acting on these L-type Ca²⁺ transporters or does the AdipoR2 have an independent regulatory pathway whereby it insulin sensitizes the alpha cell? To further investigate, cultured InR1G9's will be treated with and without recombinant adiponectin or AdipoRon to blot for changes in downstream targets. These treated, cultured alpha cells will also be used to assess transcriptional regulation of glucagon.

Diet induced obesity studies still need to be performed on these mice. Alternatively, we can use alpha cell specific deletion of the adiponectin receptors in a diet induced obesity mouse model. Utilizing either hyperinsulinemic-hypoglycemic clamps or pancreatic perfusions will be needed to assess adiponectin regulated insulin signaling within the alpha cell of these models. The loxp-flanked TdTomato reporter will be crossed onto the WT and AdipoR2 overexpression model to label alpha cells for sorting. FACS sorted alpha cells will be used to measure sphingolipid levels and transcriptional factors involved in the adiponectin and insulin signaling pathways.

The cell data exhibiting FGF21 independent lowering effects of ceramide and glucagon

secretion needs further elucidation. If lipid oxidation is occurring, by which pathway is FGF21 achieving this? In vitro, ceramidase activity and phosphatase activity assays will be used to measure increases in innate ceramide degradation or via a downstream signaling target. A timecourse of recombinant FGF21 exposure in cultured alpha cells can also be used to see acute and long term effects to help reveal this molecular pathway.

Beta-klotho deficient mice will be utilized in pERK IF, to see if impairing FGF21 signaling within the alpha cell interrupts the phosphorylation of this protein. During hyperinsulinemic-hypoglycemic clamp, to remove effects of endogenous insulin being produced, we will infuse recombinant adiponectin or FGF21 in WT or PPG KLB KO mice to assess whether either is sufficient to rescue the hypersecretory phenotype. Also, simple fasting/refeeding experiments need to be performed to evaluate regulation of glucagon and insulin in this canonical fasting hormone. Histology is needed to assess islet size and morphology in both mouse models. To evaluate minute to minute secretion of glucagon and insulin secretion in low, normal, and high glucose conditions, pancreatic perfusions will be performed in PPG KLB KO and WT mice, with and without C2 ceramide.

The results from each of these separate studies can make strides towards alternative therapeutics to regulate the glucagon to insulin ratio in both Type 1 and Type 2 diabetes. With minimal treatments for Type 1 diabetes and with occurrences of Type 2 diabetes on the rise, an alternative or supplementary approach to insulin therapies needs to be aggressively explored. These collective studies suggest that targeting the alpha cell to blunt glucagon secretion or blockade of its receptors could advance treatments of the diabetic phenotypes.